

AD-785 595

NOISE ABATEMENT AND INTERNAL VIBRA-  
TIONAL ABSORPTION IN POTENTIAL  
STRUCTURAL MATERIALS

S. A. Kulin, et al

ManLabs, Incorporated

Prepared for:

Advanced Research Projects Agency  
Army Materials and Mechanics Research Center

August 1974

DISTRIBUTED BY:

**NTIS**

**National Technical Information Service**  
**U. S. DEPARTMENT OF COMMERCE**  
5285 Port Royal Road, Springfield Va. 22151

ACCESSION for	
DTIS	White Section <input checked="" type="checkbox"/>
D+C	Blue Section <input type="checkbox"/>
UNANNOUNCED	<input type="checkbox"/>
JUSTIFICATION	
BY	
DISTRIBUTION/AVAILABILITY CODES	
DISC.	AVAIL. REQ. OR SPECIAL
A	

The view and conclusions contained in this document are those of the authors and should not be interpreted as necessarily representing the official policies, either expressed or implied, of the Defense Advanced Research Projects Agency of the U. S. Government.

Mention of any trade names or manufacturers in this report shall not be construed as advertising nor as an official indorsement or approval of such products or companies by the United States Government.

#### DISPOSITION INSTRUCTIONS

Destroy this report when it is no longer needed.  
Do not return it to the originator.

UNCLASSIFIED

SECURITY CLASSIFICATION OF THIS PAGE (When Data Entered)

REPORT DOCUMENTATION PAGE		READ INSTRUCTIONS BEFORE COMPLETING FORM
1. REPORT NUMBER AMMRC CTR74-53	2. GOVT ACCESSION NO.	3. RECIPIENT'S CATALOG NUMBER <b>AD-785 595</b>
4. TITLE (and Subtitle) Noise Abatement and Internal Vibrational Absorption in Potential Structural Materials		5. TYPE OF REPORT & PERIOD COVERED Semi-Annual Report 1 December 1973-1 June 1974
7. AUTHOR(s) S. A. Kulin, L. Kaufman, P. P. Neshe		6. PERFORMING ORG. REPORT NUMBER
9. PERFORMING ORGANIZATION NAME AND ADDRESS		8. CONTRACT OR GRANT NUMBER(s) DAAG46-74-C-0048
11. CONTROLLING OFFICE NAME AND ADDRESS Army Materials and Mechanics Research Center Watertown, Massachusetts 02172		10. PROGRAM ELEMENT, PROJECT, TASK AREA & WORK UNIT NUMBERS D/A Project: ARPA 2555 AMCMS Code: 690000.21.10846 Agency Accession: DAOE 4778
14. MONITORING AGENCY NAME & ADDRESS (if different from Controlling Office)		12. REPORT DATE August 1974
		13. NUMBER OF PAGES <b>45</b>
		15. SECURITY CLASS. (of this report) Unclassified
		15a. DECLASSIFICATION/DOWNGRADING SCHEDULE
16. DISTRIBUTION STATEMENT (of this Report)  Approved for public release; distribution unlimited.		
17. DISTRIBUTION STATEMENT (of the abstract entered in Block 20, if different from Report)		
18. SUPPLEMENTARY NOTES		
19. KEY WORDS (Continue on reverse side if necessary and identify by block number) Damping Noise reduction Vibration damping Martensitic transformations Magnetostriiction Reproduced by NATIONAL TECHNICAL INFORMATION SERVICE U S Department of Commerce Springfield VA 22151		
20. ABSTRACT (Continue on reverse side if necessary and identify by block number) The damping capacity of NiTi, Cu-Al-Ni and Fe-Pt alloys is being studied as a function of temperature above and below $M_s$ . Measurements of heat capacity and transformation characteristics have been completed for NiTi and one Fe-Pt alloy and are in progress for a second Fe-Pt alloy and the Cu-Al-Ni alloy. Mechanical property measurements and assessment of the effects of elastic and plastic strains on the characteristics of the Ni-Ti alloy are in progress. The transformation in NiTi alloys is thermoelastic. A plastic		

DD FORM 1 JAN 73 1473

EDITION OF 1 NOV 63 IS OBSOLETE

UNCLASSIFIED

SECURITY CLASSIFICATION OF THIS PAGE (When Data Entered)

UNCLASSIFIED

SECURITY CLASSIFICATION OF THIS PAGE(When Data Entered)

Block No. 20 (continued).

deformation can be employed to alter the transformation characteristics.

Measurements of electrical resistance as a function of temperature were used to characterize the transformation in Ni-Ti, follow the changes during multiple temperature cycling and establish procedures for establishing stable behavior by means of multiple cycling. The effects of deformation by rolling on the transformation characteristics of NiTi have been established.

The damping behavior of NiTi was measured on a sample whose transformation characteristics were stabilized by seventy cycles. These characteristics indicate that damping increases above  $M_s$  in the premartensitic or "soft-mode" range. Measurements of Young's modulus and heat evolution conducted on similar samples over a wide temperature range support these results. Initial experiments in the Fe-Pt system have shown that the acoustical absorption is increased greatly by ordering the parent phase prior to transformation.

UNCLASSIFIED

SECURITY CLASSIFICATION OF THIS PAGE(When Data Entered)

ja

(1) Summary of Work to Date

At present NiTi, Cu-Al-Ni and Fe-Pt alloys are being studied to determine damping capacity as a function of temperature both above and below the  $M_s$  temperature. Measurements of heat capacity and transformation characteristics have been completed for NiTi and one Fe-Pt alloy and are in progress for a second Fe-Pt alloy and the Cu-Al-Ni alloy. Mechanical property measurements and assessment of the effects of elastic and plastic strains on the characteristics of the Ni-Ti alloy are in progress.

It was found that the martensitic transformation in NiTi alloys is of the thermoelastic type. Evidence was obtained which indicated a large increase in internal damping capacity at temperatures associated with the premartensitic or "soft-mode" temperature regime. Experiments completed during the past three months have confirmed these findings. Moreover it was found that plastic deformation can be employed to substantially alter the transformation characteristics. Consequently it is anticipated that a corresponding change in damping characteristics is attainable. It was also determined that the damping capacity in Fe-Pt alloys is directly related to the amount of ordering in the parent phase.

(2) Program Objectives

The objective of this interdisciplinary program is to obtain a basic understanding of the mechanism of high internal damping in alloys which undergo certain martensitic-type transformations and thereby to identify potential structural materials approaches for use in noise and vibration abatement applications.

(3) Major Accomplishments

During this reporting period it was ascertained that the transformation in NiTi did not produce acoustic emissions nor were such effects noted in the premartensitic instability temperature range above  $M_s$ . This indicates a thermoelastic type of transformation associated with the high internal damping factor.

The resonant dwell apparatus for damping factor determination has been modified to operate over a temperature range below and above ambient temperatures.

Initial experiments in the Fe-Pt system have shown that the acoustical absorption is increased greatly by ordering the parent phase prior to transformation.

Measurements of electrical resistance as a function of temperature have been employed to characterize the transformation in Ni-Ti, follow the changes during multiple temperature cycling and establish procedures for establishing stable behavior by means of multiple cycling. The effects of 3, 7 and 15% deformation by rolling on the transformation characteristics of NiTi has been established.

The damping behavior of NiTi was measured on a sample whose transformation characteristics were stabilized by seventy cycles. These characteristics clearly indicate that damping occurs above the  $M_s$  temperature in the premartensitic or "soft-mode" range. Measurements of Young's modulus and heat evolution conducted on similar samples over a wide temperature range support the results obtained in the damping studies.

(4) Problems Encountered

All subcontracts have been negotiated.

(5) Fiscal Status

5.1 Amount provided for contract:	\$99,868
5.2 Expenditures to date:	65,848
5.3 Funds required to complete the work:	34,020
5.4 Estimated date of completion of work:	September 1, 1974

(6) Action Required by ARPA or the Contract Agent

It is requested that the proposed continuation of this study be funded as soon as possible to facilitate the continuity of effort.

(7) Future Plans

No significant changes are planned in the course of the work in this program.

## I. INTRODUCTION

Military and civilian agencies are confronted with many problems related to the reduction of noise and vibration. Military concern is focused on tactical and psychological advantages; civilian concern is addressed to social and economic problems. This report summarizes the progress during the first six-month period of an interdisciplinary program on noise and vibration abatement in potential structural materials. The cooperating groups in this program include the Metallurgy Department of M.I.T., the Physics of Solids Group at the Army Materials and Mechanics Research Center, an acoustical group at Bolt, Beranek and Newman, Inc. and a physical metallurgy group at ManLabs, Inc. The initial objective of this program is to obtain a basic understanding of the mechanisms for achieving high internal damping and thereby to identify potential materials approaches in noise and vibration reduction technology.

## II. PROGRAM ACTIVITIES IN THE FIRST SIX MONTHS

### A. Seminar Series on Martensitic Transformations

During this initial period extensive discussions were held on the relationship between martensitic transformation characteristics and damping. Attention was focused on NiTi, Fe-Pt, and Cu-Al. During the month of January 1974 a series of formal seminars was held in conjunction with the MIT-IAP program at which this discussion was continued. A copy of this seminar program is given below.

#### SEMINARS ON MARTENSITIC TRANSFORMATIONS

Month of January 1974

Mondays, Wednesdays, Fridays: 9:30 - 12:30  
Room 13-5002

<u>Monday, 7 January.</u>	G. B. Olson, "Spontaneous Nucleation"
<u>Wednesday, 9 January.</u>	G. B. Olson, "Strain-Induced Nucleation"
<u>Friday, 11 January.</u>	G. A. Knorovsky, "Autocatalytic Nucleation"
<u>Monday, 14 January.</u>	
<u>Wednesday, 16 January.</u>	P. Clapp, "Soft-Mode Transformations"
<u>Friday, 18 January.</u>	L. P. Kaufman, "Thermodynamics of the Iron-Platinum and Copper-Aluminum Systems"
<u>Monday, 21 January.</u>	W. S. Owen, "Thermoelastic Martensites"
<u>Wednesday, 23 January.</u>	R. J. Salzbrenner, "Damping Phenomena in Martensitic Systems"
<u>Friday, 25 January.</u>	J. B. Vander Sande, "Carbon Clustering in Martensite"

Participants: J. W. Cahn, P. Clapp, M. Cohen, N. J. deCristofaro, B. Djuric, S. S. Hansen, R. Kaplow, L. P. Kaufman, G. A. Knorovsky, S. A. Kulin, H. Matsueda, G. B. Olson, W. S. Owen, K. C. Russell, A. K. Sachdev, R. J. Salzbrenner, J. B. Vander Sande, R. J. Weiss.

### B. ManLabs Activities

ManLabs activities during this reporting period have been directed toward establishing whether the damping phenomena observed in NiTi is directly related to the onset of transformation or if it occurs in a temperature range above  $M_s$  where atomic



shuffles are thought to take place. In order to test the latter hypothesis it was decided to perform simultaneous measurements of the electrical resistance and acoustic emission of NiTi samples as a function of temperature. The measurements were conducted on the standard "reed" samples which BBN requires for measurements of damping capacity as a function of temperature. The resistivity of a typical NiTi 55 a/o alloy is shown in Figure 1 as a function of temperature cycling through the transition range. Simultaneous metallographic and resistance measurements do not disclose actual formation of the daughter phase in the region where the resistance increases. This is where the "atomic shuffles" are supposed to take place. In order to determine if these "soft mode displacements" lead to enhanced damping, specimens were temperature cycled many times to obtain a well defined resistivity peak. The peak in the cooling curve represents the  $M_s$  temperature as defined by the temperature at which the first observable surface relief forms on cooling (1-3).\*

Preliminary results obtained by BBN indicate that the increase in damping capacity begins in the temperature regime above  $M_s$  corresponding to the region of increasing electrical resistivity during cooling of the NiTi alloy.

In order to perform the above type experiments, a precision electrical resistivity apparatus was constructed using the double Kelvin Bridge principle. This apparatus uses an L&N type K-3 potentiometer, a standard cell, constant voltage supply, a regulated power supply, a L&N resistance standard, and a L&N D.C. null detector. The precision of measurement obtained is of the order of  $1 \times 10^{-6}$  ohm-cm.

An acoustic apparatus was designed and constructed to yield information as to the types of martensitic transformations occurring, i.e. burst phenomena, thermoelastic, etc. This equipment uses a wire hook-up from a crystal transducer to

---

\* Underscored numbers in parentheses denote references.

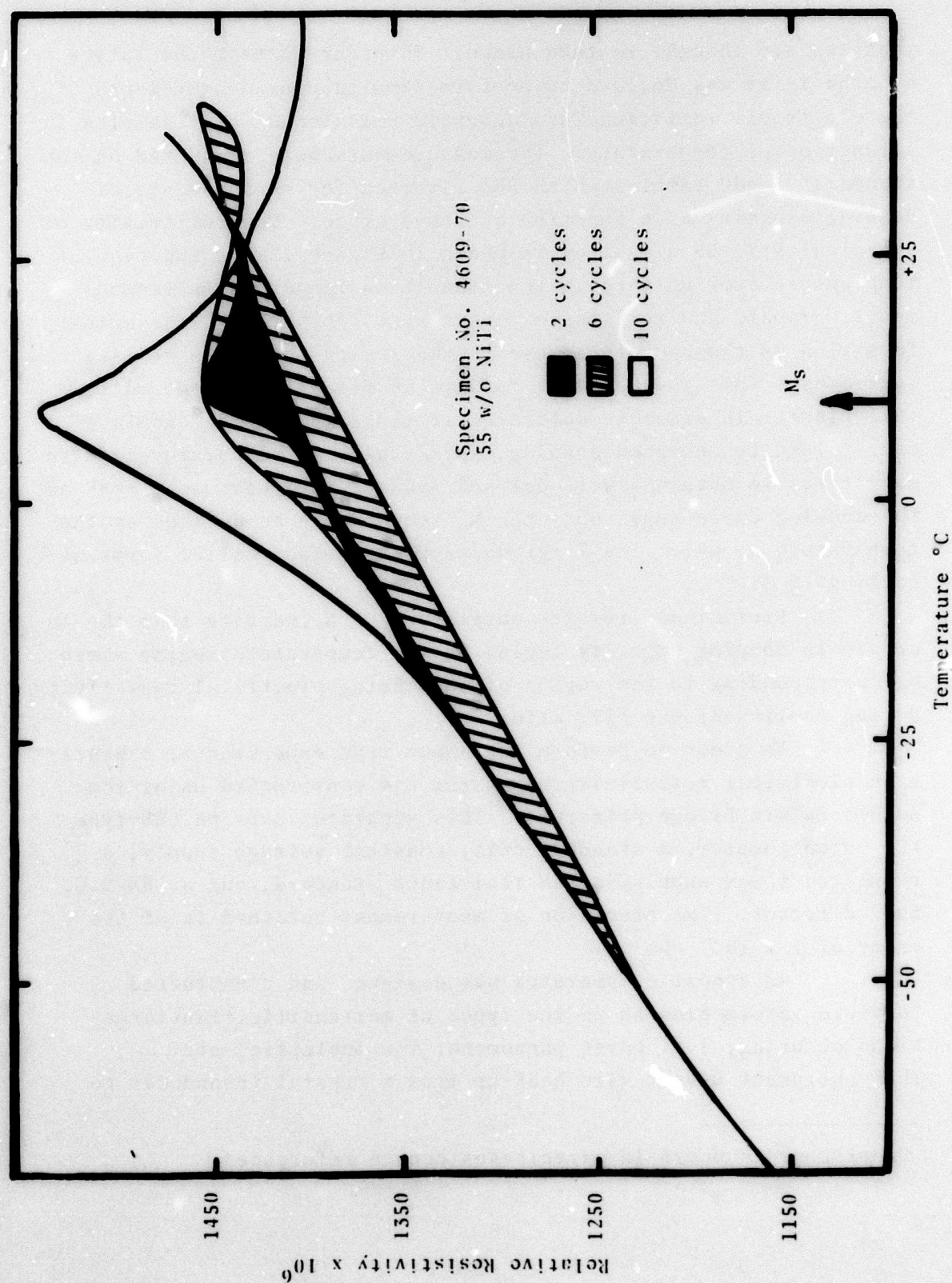


Figure 1. Electrical Resistivity versus Temperature for a 55 w/o NiTi Alloy as a Function of Number of Temperature Cycles.

the specimen. Standard amplifier and loud speaker are connected to the transducer. In addition, an Esterline Angus high speed recorder was connected so that a permanent record could be made of the acoustic emissions from the specimen during temperature cycling through the temperature range of interest. No acoustic emissions have been observed to date in experiments performed on NiTi samples as cycled through the "soft mode" and the martensitic transformation temperature ranges. In contrast, much acoustic activity was detected during transformation in experiments using 70 Fe-30 Ni alloys in which "burst type" martensitic transformation is known to occur. The above experiments indicate that the mechanism of martensitic transformation in the highly damping NiTi alloys is of the thermo-elastic mode.

In order to establish a stable transformation behavior as a baseline treatment for samples to be treated prior to various measurements, multiple temperature cycles between  $-65^{\circ}\text{C}$  and  $+90^{\circ}\text{C}$  were employed. The cycling treatment consisted of immersion in a Dow Corning 200-10CS/Dry Ice mixture held at  $-65^{\circ}\text{C}$  and a second Dow Corning 200-10CS bath at  $90^{\circ}\text{C}$ . A ten-minute cycle is employed in this treatment. Figure 2 shows the resistance-temperature curve obtained after 76 cycles. Since these characteristics are well defined, a treatment of 50-70 cycles has been selected as the basis for preparation of specimens to be evaluated by heat evolution, damping and Young's modulus measurements over the  $-65^{\circ}\text{C}$  to  $90^{\circ}\text{C}$  temperature range.

A second series of experiments designed to evaluate the effects of cold work on the transformation characteristics has been carried out. These studies were conducted by heat treating strips of 55 w/o NiTi (4866) by annealing at  $790^{\circ}\text{C}$  for thirty minutes, quenching in water and cycling between  $-65^{\circ}\text{C}$  and  $+90^{\circ}\text{C}$  fifty times. Following this treatment the electrical resistance of the 190 mil x 250 mil x 5.5 inch strip was measured as a function of temperature. Figure 3 shows the results of this test. Subsequently, the strip was deformed by rolling at room temperature. This treatment was followed by a second set of fifty temperature cycles be-

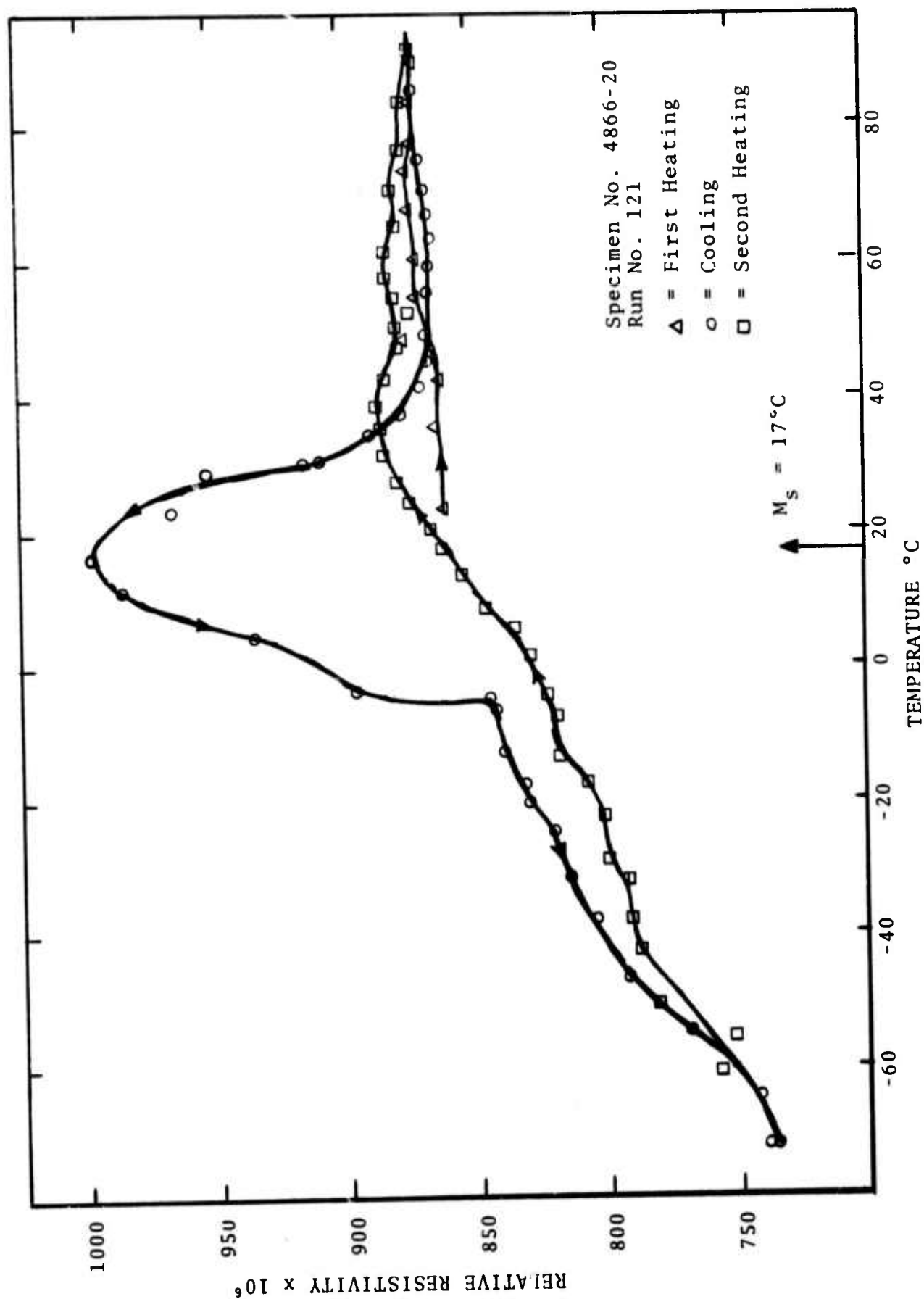


Figure 2. Electrical Resistivity versus Temperature for a 55 w/o NiTi Alloy as a Function of Temperature after 76 cycles between  $-65^\circ\text{C}$  and  $+90^\circ\text{C}$ .

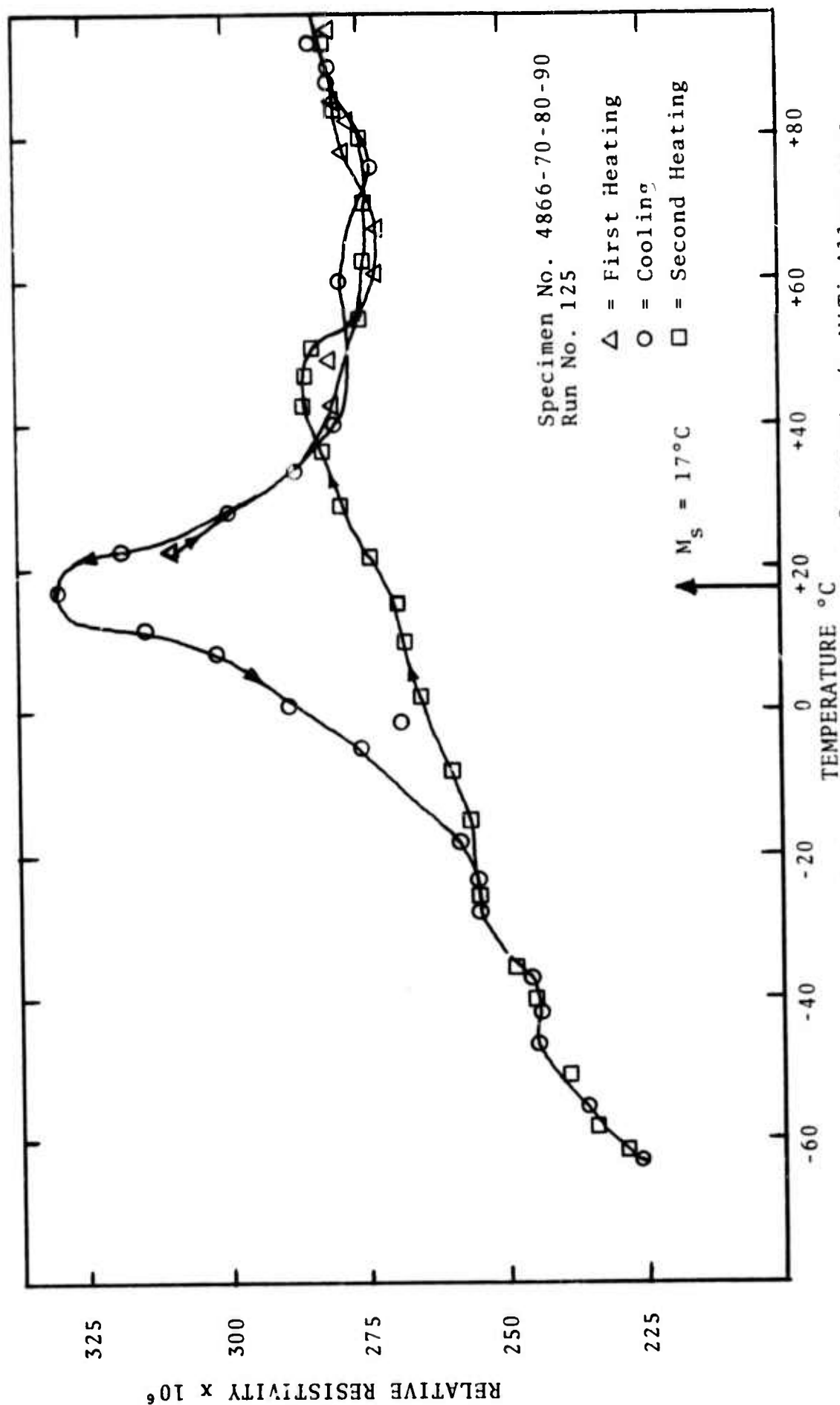


Figure 3. Electrical Resistivity versus Temperature for a 55 w/o NiTi Alloy as a Function of Temperature after 50 cycles between  $-65^\circ\text{C}$  and  $+90^\circ\text{C}$ .

tween  $-65^{\circ}\text{C}$  and  $+90^{\circ}\text{C}$ . Finally the resistance-temperature characteristics were measured again. Three levels of deformation were employed in this series of tests. These corresponded to 3.2%, 7% and 15.2%. The resultant measurements (obtained on three different bars) are shown in Figures 4-6. These curves show that deformation in the 0-7% range broadens the temperature range of the transformation while 15% deformation seems to obscure the change of resistance with transformation or eliminate the transformation entirely. These test bars will be examined by determining their damping characteristics so that the effect of deformation on damping can be evaluated. The combined result will then be employed to determine the optimum treatment which can be employed to achieve attractive damping and strength characteristics.

Due to the difficulty in machining NiTi specimens, it was decided to determine the possible usefulness of a flat-type specimen as compared with the standard reed-type specimens employed for damping capacity measurements in the BBN Resonant Dwell Apparatus. Specimens of each type were fabricated and were temperature cycled (up to 76 cycles) to yield stable temperature resistivity curves prior to measurement of damping capacity as a function of temperature by BBN. The results of the damping studies on the flat-type specimens did not compare favorably with the standard reed-type samples. As a consequence, the latter configuration will be employed exclusively.

Five compositions of Cu-Al-Ni alloys were melted and cast into rod form for the M.I.T. program in which it is intended to grow single crystals of these alloys for fundamental studies. Four additional Nitinol alloys of different TTR characteristics in wire and sheet form were procured and are being heat treated and cold worked for preparation of samples for damping studies. The damping measurements will be carried out at BBN on reed specimens over a range of temperature as a function of thermo-mechanical treatment.

A bibliography of references related to NiTi alloys was completed and distributed to the groups in this program.



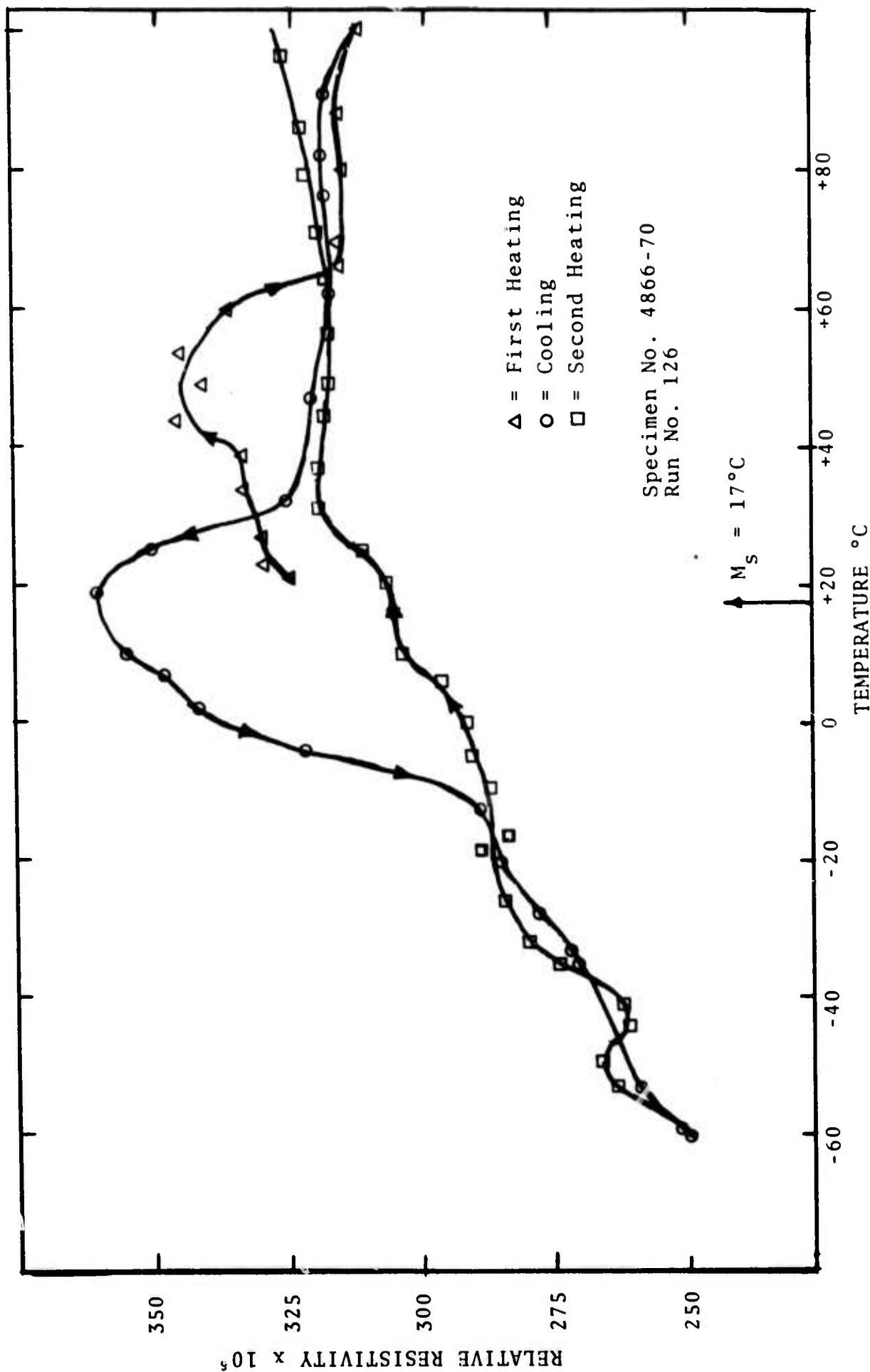


Figure 4. Electrical Resistivity versus Temperature for a 55 w/o NiTi Alloy as a Function of Temperature after 3.2% deformation by rolling followed by 50 cycles between  $-65^\circ\text{C}$  and  $+90^\circ\text{C}$ .

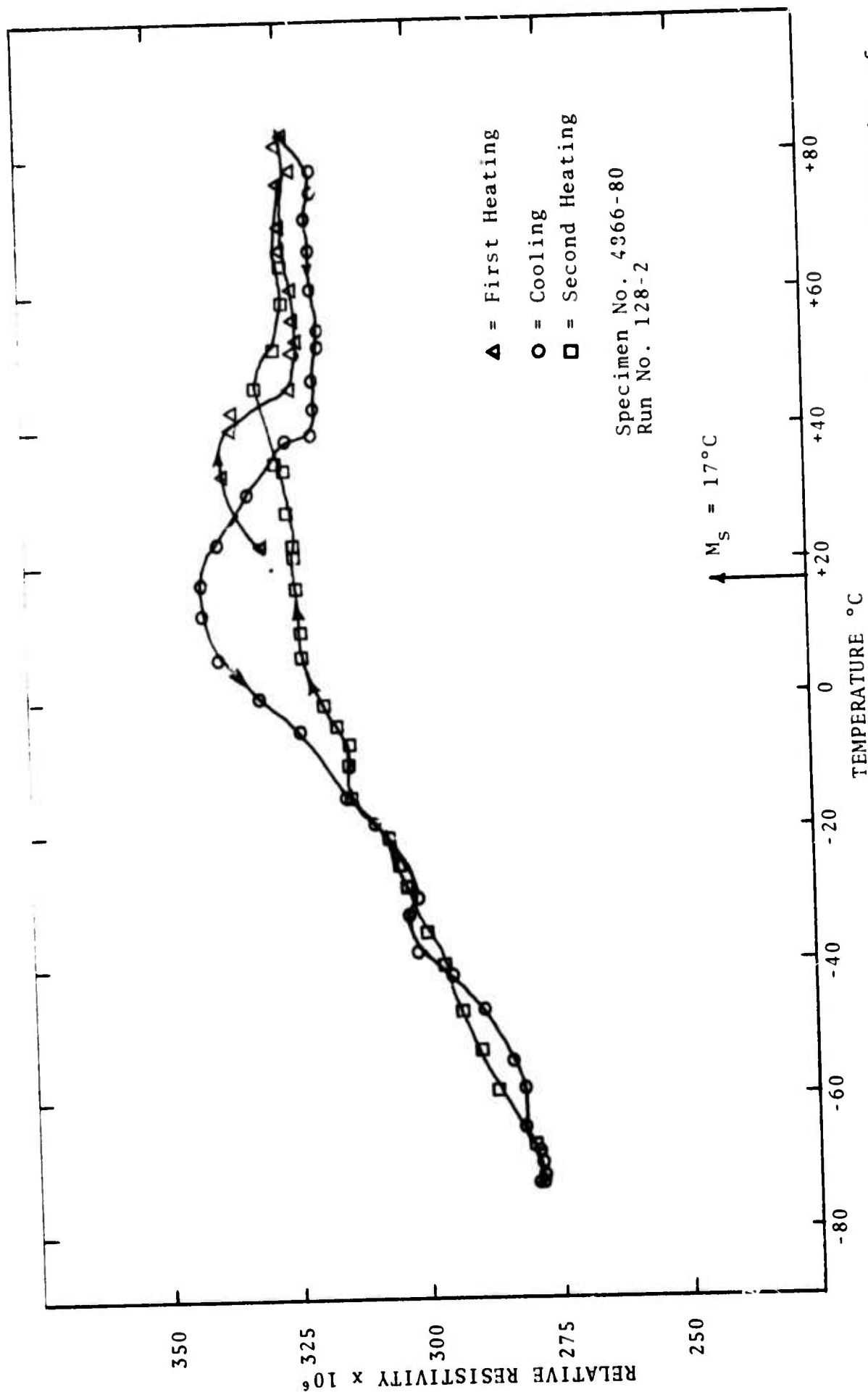


Figure 5. Electrical Resistivity versus Temperature for a 55 w/o NiTi Alloy as a Function of Temperature after 7% deformation by rolling followed by 50 cycles between  $-65^\circ\text{C}$  and  $+90^\circ\text{C}$ .



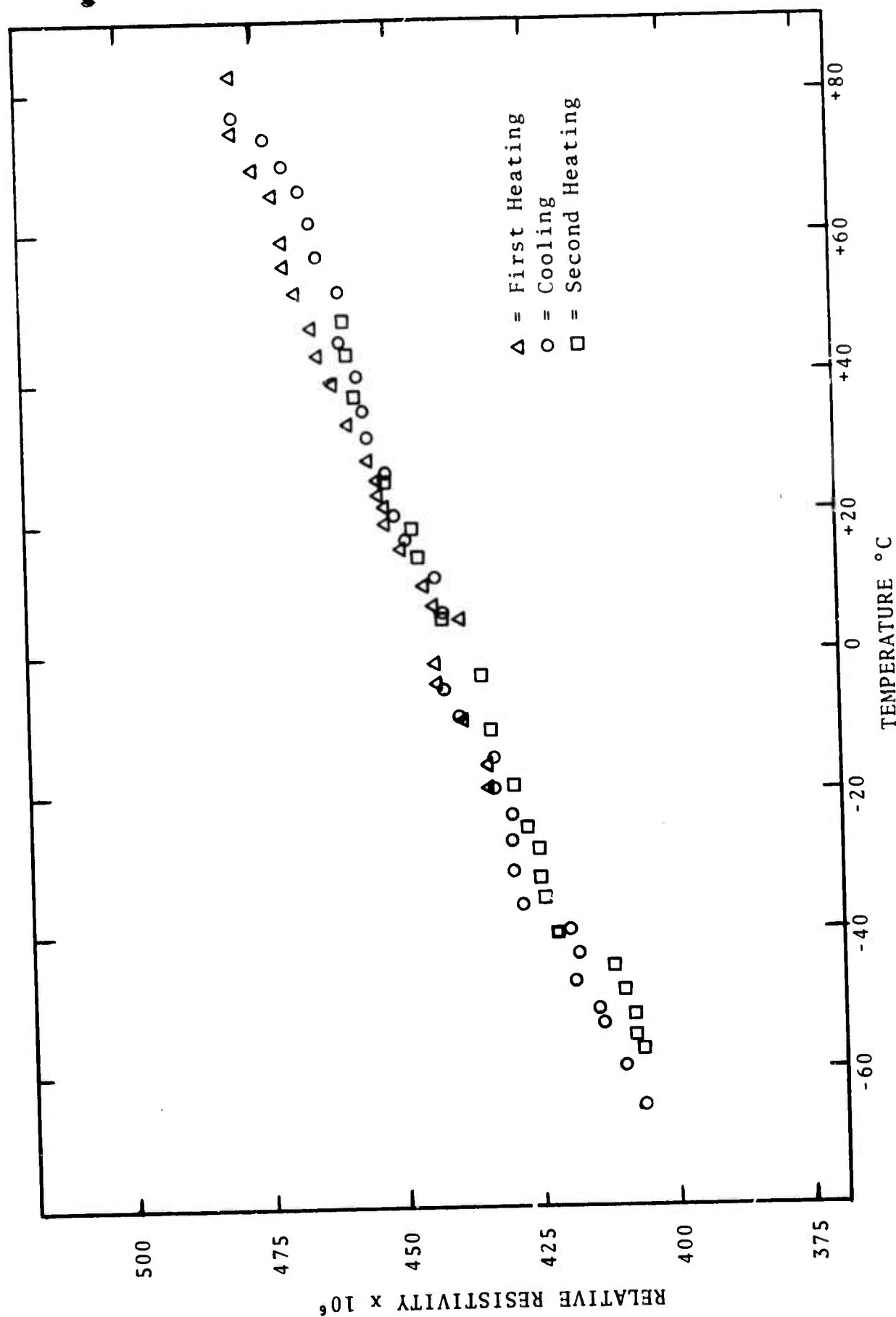


Figure 6. Electrical Resistivity versus Temperature for a 55 w/o NiTi Alloy as a Function of Temperature after 15% deformation by rolling followed by 50 cycles between  $-65^{\circ}\text{C}$  and  $+90^{\circ}\text{C}$ .

### C. M.I.T.-A.M.M.R.C. Activities

The M.I.T. and A.M.M.R.C. activities have concentrated on thermo-elastic transformations in  $\text{Fe}_3\text{Pt}$  and  $\text{Cu}_3\text{Al}$ . In addition, measurement of heat evolution, Young's modulus and damping have been performed on NiTi samples which were exposed to multiple cycles to stabilize the transformation characteristics. In the  $\text{Cu}_3\text{Al}$  case loss factors up to  $1500 \times 10^{-4}$  ( $Q^{-1}$ ) have been observed. These loss factors can be altered by appropriate temperature cycling. They also seem to exhibit peaks as a function of temperature as shown schematically in Figure 7. In these cases it is not clear whether the peak is directly associated with  $M_s$ . However, the present study should clear up this matter. It should be pointed out that the figure shows  $Q^{-1}$  versus  $T$  as determined in a torsional pendulum at low frequency and stress levels.

Preliminary, crude experiments indicated clearly that the acoustical absorption of  $\text{Fe}_3\text{Pt}$  is increased greatly by ordering the parent phase before transformation. All the other known high-damping-capacity martensitic alloys are also ordered. Thus we are studying ordering in  $\text{Fe}_3\text{Pt}$ , the effects this has on the kinetics of the nucleation and growth of martensitic plates and on the physical properties of the two-phase product, and the ways in which these order-induced changes in structure and physical properties affect acoustical absorption. It is known from earlier work that stoichiometric  $\text{Fe}_3\text{Pt}$  undergoes a paramagnetic-ferromagnetic transition in the austenitic state, the Curie temperature increasing with the degree of order. This alloy exhibits a large Invar dilation on passing through the Curie temperature. It also has a sharp internal friction peak in the vicinity of the Curie temperature and the martensite formed from ferromagnetic austenite is thermoelastic. It is possible, of course, that all these changes in physical properties induced by changing the order in the  $\gamma$ -phase are interrelated, but details of the interactions are not known. In particular, although it is conceivable that in order to achieve high damping the martensite must be capable of reversible thermo-

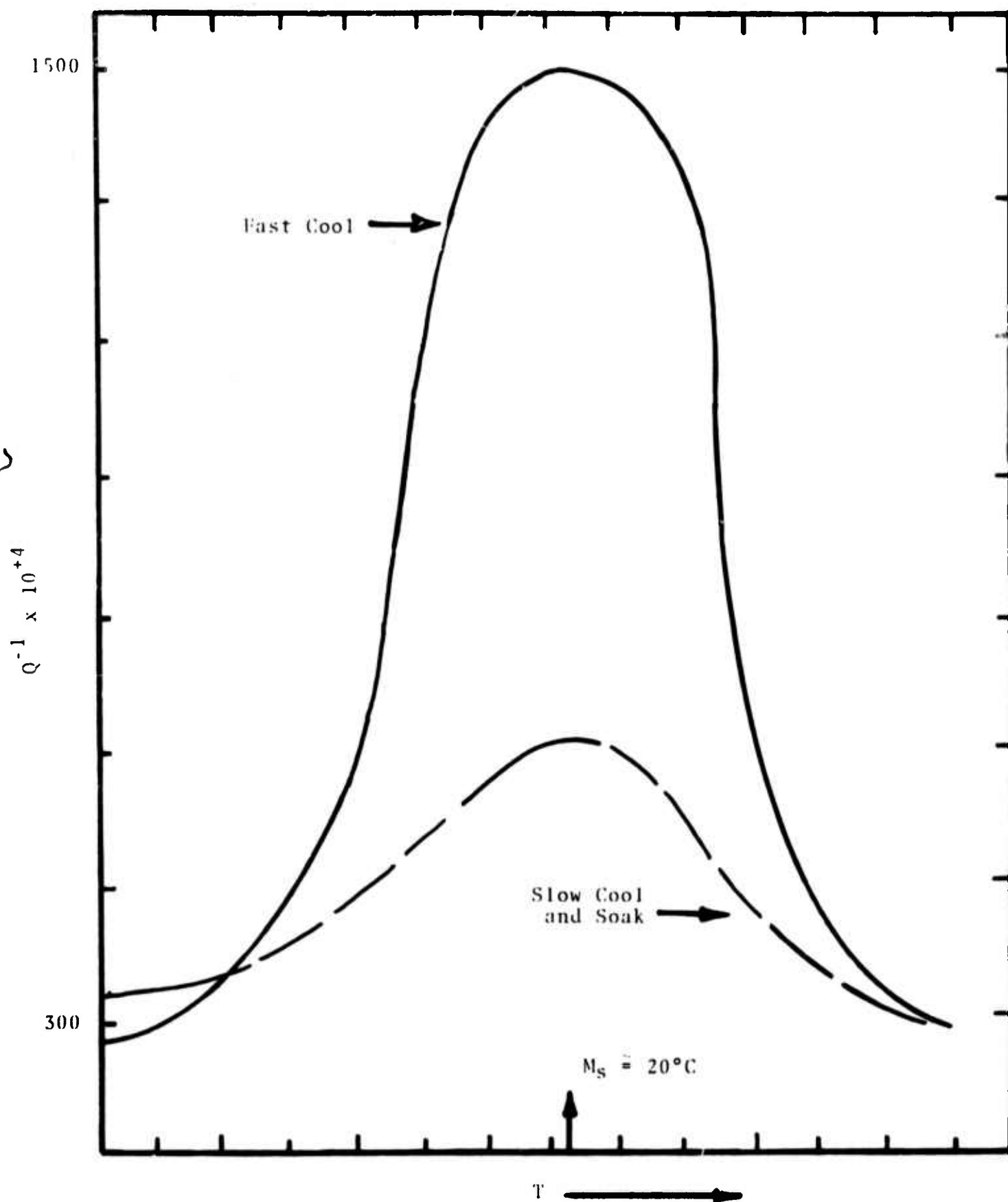


Figure 7. Schematic Diagram of Damping Factor versus Temperature for a Cu-Al-Ni Alloy.

elastic growth, this has not been demonstrated experimentally and the structural factors promoting thermoelastic growth are not understood sufficiently to provide a basis for the design of high damping-capacity alloys.

The initial evaluation of  $\text{Fe}_3\text{Pt}$  carried out under the present contract was designed to examine the ordering process in  $\text{Fe}_3\text{Pt}$  by X-ray diffraction and transmission electron microscopy to determine the influence of the degree of order of the  $\gamma$ -phase on the martensitic transformation by measuring the enthalpy of transformation in a differential calorimeter and calculating the free energy driving the process, and to determine the influence of the degree of order on the damping properties and on the mechanical strength of the alloy.

The first experiments have been done on an iron-25.2a/o platinum alloy. In order to achieve a completely disordered structure, various quenching procedures were tried, but in all instances a certain degree of order remained in the specimens. It seems that the ordering reaction is very fast and cannot be suppressed by applied quenching rates.

The ordering process of this alloy is complex. After short annealing times, besides the superlattice lines of the ordered  $\text{Fe}_3\text{Pt}$  phase, some other diffraction lines appear. They at first become stronger with increasing annealing time, but eventually disappear, leaving only the lines of the ordered  $\text{Fe}_3\text{Pt}$  phase. It was possible to index the new lines as belonging to a tetragonal face-centered cubic lattice, corresponding to the  $\text{FePt}$  structure.

A series of samples ordered various times at  $625^\circ\text{C}$  were examined in a scanning differential calorimeter in order to evaluate the enthalpy of martensitic transformation. It was also possible to determine the  $M_s$  temperature by the same method. The results show that the  $M_s$  temperature decreases with ordering time, dropping to about  $100^\circ\text{K}$  after four hours at  $625^\circ\text{C}$ . Since this was the lower limit of the calorimeter, the samples with higher degrees of order could not be measured.

Detailed X-ray and metallographic work conducted during

the past three months has shown that on quenching from above 900°C an ordered tetragonal phase based on FePt is nucleated at austenitic grain boundaries. On subsequent annealing at 625°C, this phase grows simultaneously with the ordering of the Fe<sub>3</sub>Pt cubic phase within the grains. At an intermediate stage of annealing the tetragonal phase, based on a CuAu I-type structure, spreads over the whole specimen. This phase is metastable, however, and on prolonged annealing at 625°C it disappears, being replaced by cubic, ordered Fe<sub>3</sub>Pt. The sequence in which the tetragonal FePt and cubic Fe<sub>3</sub>Pt phases appear on annealing is the same in the 25 and 27 a/o Pt alloys, but both ordering processes are slower in the latter alloy.

The metastable tetragonal phase in both alloys has the same lattice parameter ( $a = 3.850\text{\AA}$ ,  $c = 3.715\text{\AA}$ ) which does not change with time of annealing. These cell dimensions are the same as for the stable ordered FePt phase found in alloys with between 32 and 62 a/o Pt. The lattice parameter of the cubic Fe<sub>3</sub>Pt increases gradually during the ordering process (from  $3.722\text{\AA}$  to  $3.734\text{\AA}$  in the 25 a/o Pt alloy).

It is now possible to understand some earlier observations on the effect of ordering on the martensitic behavior of the 25 a/o Pt alloy. The thermoelastic and microstructural reversibility are markedly different in specimens quenched after annealing for medium and long times. The present work has shown that martensite formed on quenching specimens after medium annealing times is generated from the metastable, tetragonal AuCu I-type structure, whereas the martensite formed from well-annealed austenite originates from the cubic, ordered Fe<sub>3</sub>Pt structure. Simple experiments have indicated that the martensite produced from the cubic phase has a high damping capacity. The relative magnitude of the damping effect in martensite formed from the metastable tetragonal phase is unknown as yet. The damping in these Fe-Pt martensites will be studied more systematically with the BBN equipment and by ultrasonic attenuation methods.

The initial activities on the Cu-base alloys have been directed

towards finding compositions which result in ordered thermoelastic martensite after suitable thermal treatment. Alloys of Cu-Ni with a range of Al contents have been made up in an induction furnace. The alloys range from 12.0 to 14.3 w/o Al with 3.0 w/o Ni and the remainder Cu. Single crystals of Cu-14.0Al-3.0Ni and Cu-12.9Al-3.0Ni have been grown in an induction zone-refining furnace.

Samples of Cu-14.0Al-3.0Ni and Cu-14.1Al-3.0Ni have been run on a differential thermal calorimeter at AMMRC. Critical results indicate that the  $M_s$  of the sample can be determined quite well by calorimetry. Small samples (approximately 20mg) indicated that the  $\beta_1 + \gamma_1$  martensitic reaction occurs in a very narrow temperature range- less than  $0.07^\circ\text{C}$  between the  $M_s$  and  $M_f$  for the samples tested (indicated from measurements made at the slowest rate of temperature change allowed on the machine used). Larger samples ( $\sim 120\text{mg}$ ) showed a difference of  $\sim 5.0^\circ\text{C}$  between  $M_s$  and  $M_f$ . This may show the effect of the larger samples (bulk) matrix on the thermoelastic transformation. In both large and small samples there is an appreciable difference between  $A_s$  and  $A_f$  (about  $15^\circ\text{C}$ ) and the heat liberated versus temperature curve exhibits a significant amount of structure. The complexity of the transformation curves will be better understood after further optical study of the transformations.

Samples of Cu-14.0Al-3.0Ni single crystals have been polished and optically examined. The reported color change has been observed to occur in the transformation of  $\beta_1' + \gamma_1'$  ( $\beta_1$  is an ordered BCC phase and is copper-red in color;  $\gamma_1'$  is basically an ordered HCP structure and is a yellowish-gold in color). A sample of the  $\beta_1$  (parent) phase was transformed under an optical microscope by adding liquid nitrogen to the glass dish holding the sample. The martensite phase was seen to grow into the parent phase in a slow (thermoelastic) manner. The martensite plates were seen to retract in a similar manner when the sample was reheated above  $A_s$ . A thermal recycling of the  $\beta_1 + \gamma_1'$  transformation indicated that the microstructure did not have a "memory." The lack of a "microstructural memory" may be due to the rapid and erratic manner in which the sample was thermally cycled.

In order to gain some idea of possible mechanisms which contribute to high damping in the thermoelastic alloys, a simple stressing device was constructed. A Cu-Al-Ni sample was stressed about 200 psi in compression and observed simultaneously under a low-power light microscope. As the sample was stressed, twins could be seen to appear and to increase in length and number as the stress was increased. These same twins disappeared immediately upon the release of the stress. The interface between the  $\gamma_1'$  martensite and the  $\beta_1$  parent phase was allowed to move upon the application of an applied stress. The amount of  $\gamma_1'$  increased with the applied stress. After the stress was removed, the  $\gamma_1' + \beta_1$  interface retracted slightly, but did not fully recover its original unstressed position. These optical studies are continuing.

Several runs of damping (specimen loss factor =  $g_s$ ) versus temperature have been performed on a standard machined sample of NiTi. These runs were conducted on the Resonant Dwell Apparatus belonging to Bolt, Beranek and Newman. Attention has been paid to improving the experimental technique and equipment set-up. Since progress has been made in improving the reliability of the data, damping measurements on Cu-Al-Ni should be carried out in the near future.

The BBN resonant dwell apparatus generates damping ( $g_s \equiv Q^{-1}$ ) versus temperature curves. The applied bending stress is between 1 and 10 ksi, and the frequency is between 100 and 1000 Hz. Experimentally, it was found that the damping varies with the cycling of the temperature-control unit, but the quality of the measurements could be improved significantly by determining the damping isothermally versus strain amplitude (tip deflection). This involves measuring the resonant frequency and the accelerometer output as a function of controlled tip displacement. Over the range of tip displacement,  $y_t$ , employed, the acceleration,  $a_0$ , and the resonant frequency,  $f_n$ , of the sample are each linear functions of  $y_t$  which increases confidence in the values of  $a_0$  and  $f_n$  as shown in Figure 8. The damping,  $g_s$ , is nearly independent of  $y_t$  at low values of  $g_s$ , but increases with  $y_t$  at larger values as

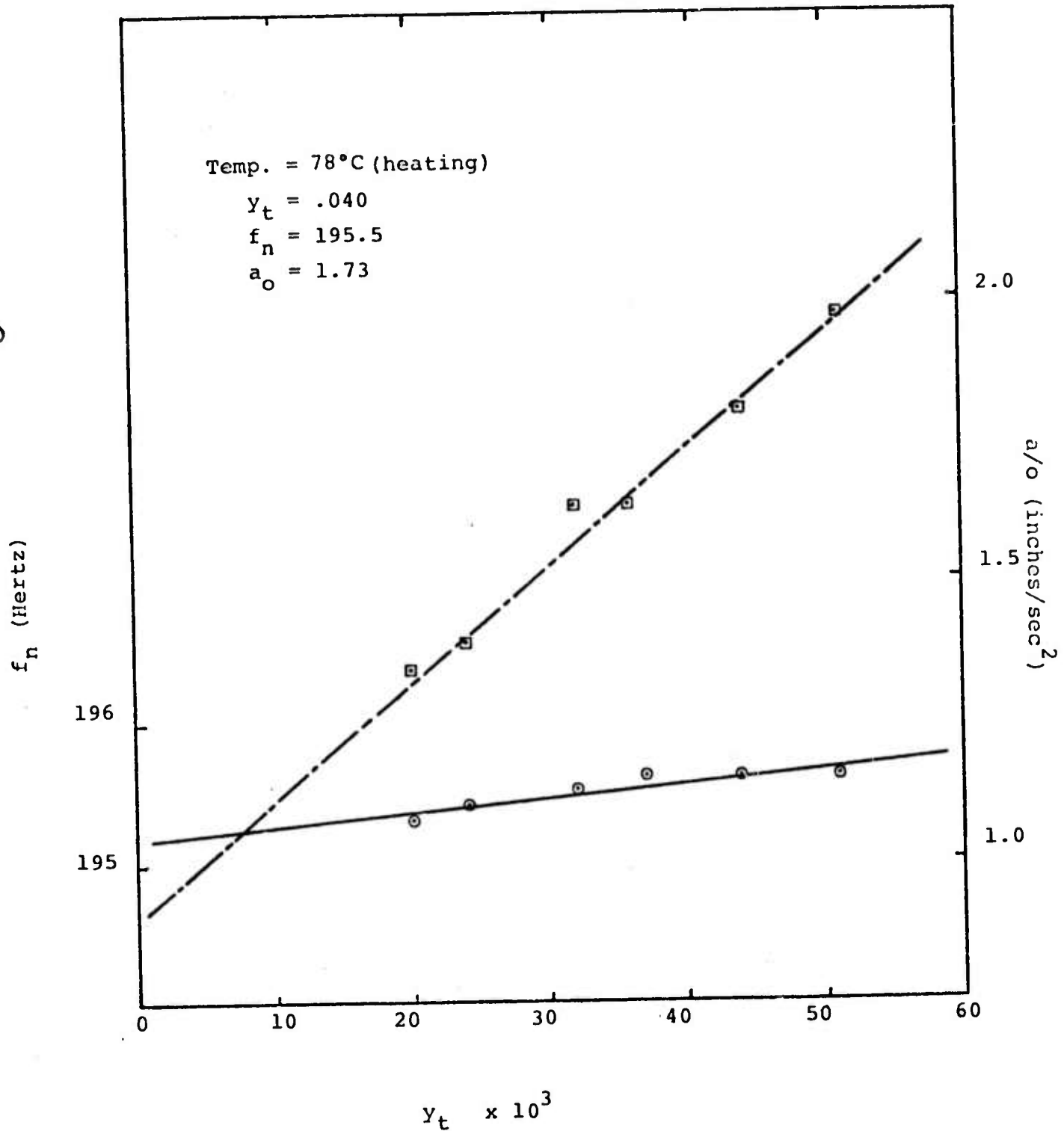


FIGURE 8. Sample resonant frequency ( $f_n$ ) and acceleration ( $a_o$ ) as a function of tip deflection ( $y_t$ ) at a temperature of 78° C.



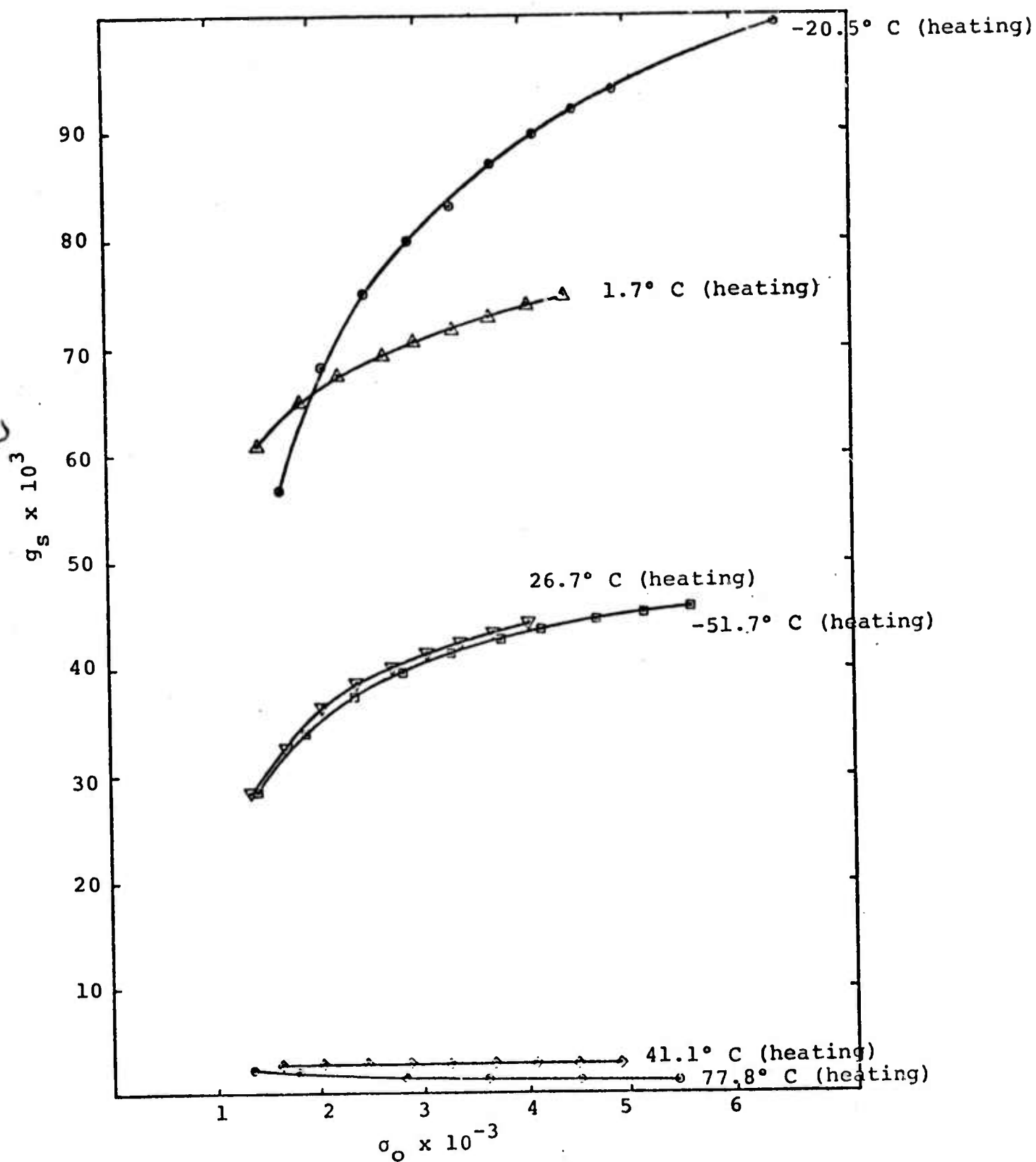


FIGURE 9. Specimen damping factor ( $g_s$ ) as a function of maximum bending stress ( $\sigma_o$ ) at various temperatures.

illustrated in Figure 9.

"Isothermal" curves of  $f_n$  and  $a_0$  versus  $y_t$  were taken on both cooling and heating; values of  $f_n$  and  $a_0$  were selected for  $y_t = 0.040$  in. and used to calculate  $g_s (= Q^{-1})$ . All specimens were first heated to well above  $M_s$ , held for 15-30 minutes, then slowly cooled to the temperature at which the measurement was to be made, and held for 15 to 20 minutes to insure thermal equilibrium. The  $f_n$  versus  $y_t$  and  $a_0$  versus  $y_t$  data were taken by increasing  $y_t$  in a stepwise fashion at the given temperature. Each of these "isothermal" curves yields one point on the damping versus temperature plots, and since only comparatively few of these measurements can be made each day, compatibility of measurements taken on different days had to be determined. The agreement was found to be good. Figure 10 is a plot of damping versus temperature data for specimens with different stress and thermal histories. Figure 11 shows the curves for specimens heated and cooled; there is a small hysteresis.

The dynamic Young's modulus of NiTi, measured at 180Hz, was determined as a function of temperature by noting the variation in resonant frequency. These results, together with data on the change in electrical resistance and heat capacity, measured in a differential thermal calorimeter, are shown as a function of temperature in Figure 12.

On cooling, the marked increase in the damping capacity and the decrease in Young's modulus set in at the same temperature ( $\sim 45^\circ\text{C}$ ). The increases in electrical resistance and heat capacity also start together, but at a temperature ( $\sim 25^\circ\text{C}$ ) which is some  $20^\circ$  lower than the temperature at which the modulus and damping start their increase. The  $M_s$  of this alloy is, however, indicated by the peak in the resistivity curve on cooling, and this occurs at about  $5^\circ\text{C}$ . The damping thus seems to increase significantly before  $M_s$  is reached (in the unstressed sample) and this may result from (1) stress-induced martensite (i.e. the stress-induced raising of  $M_s$ ), (2) premartensitic effects in the alloy, or (3) a combination of both.

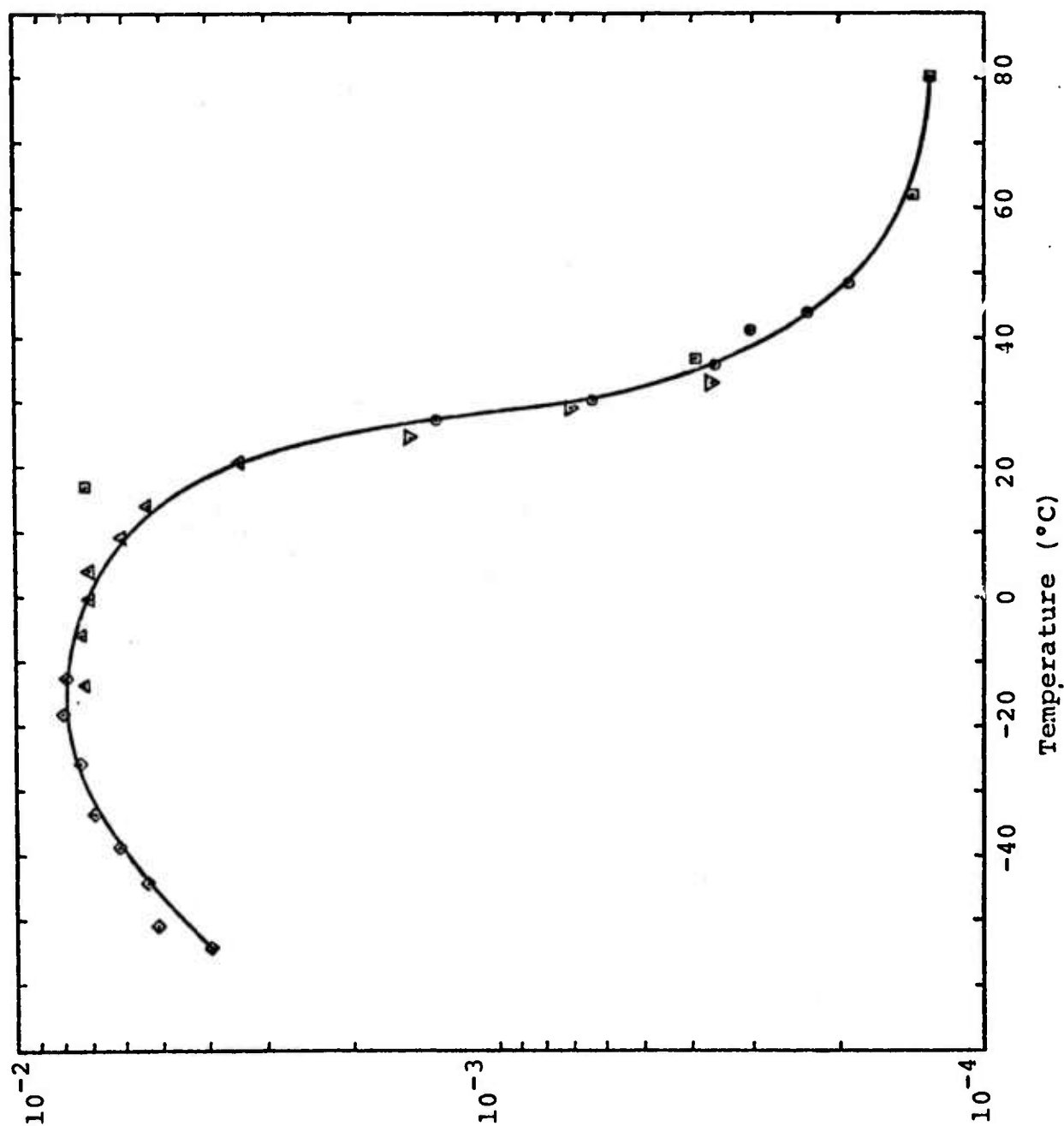
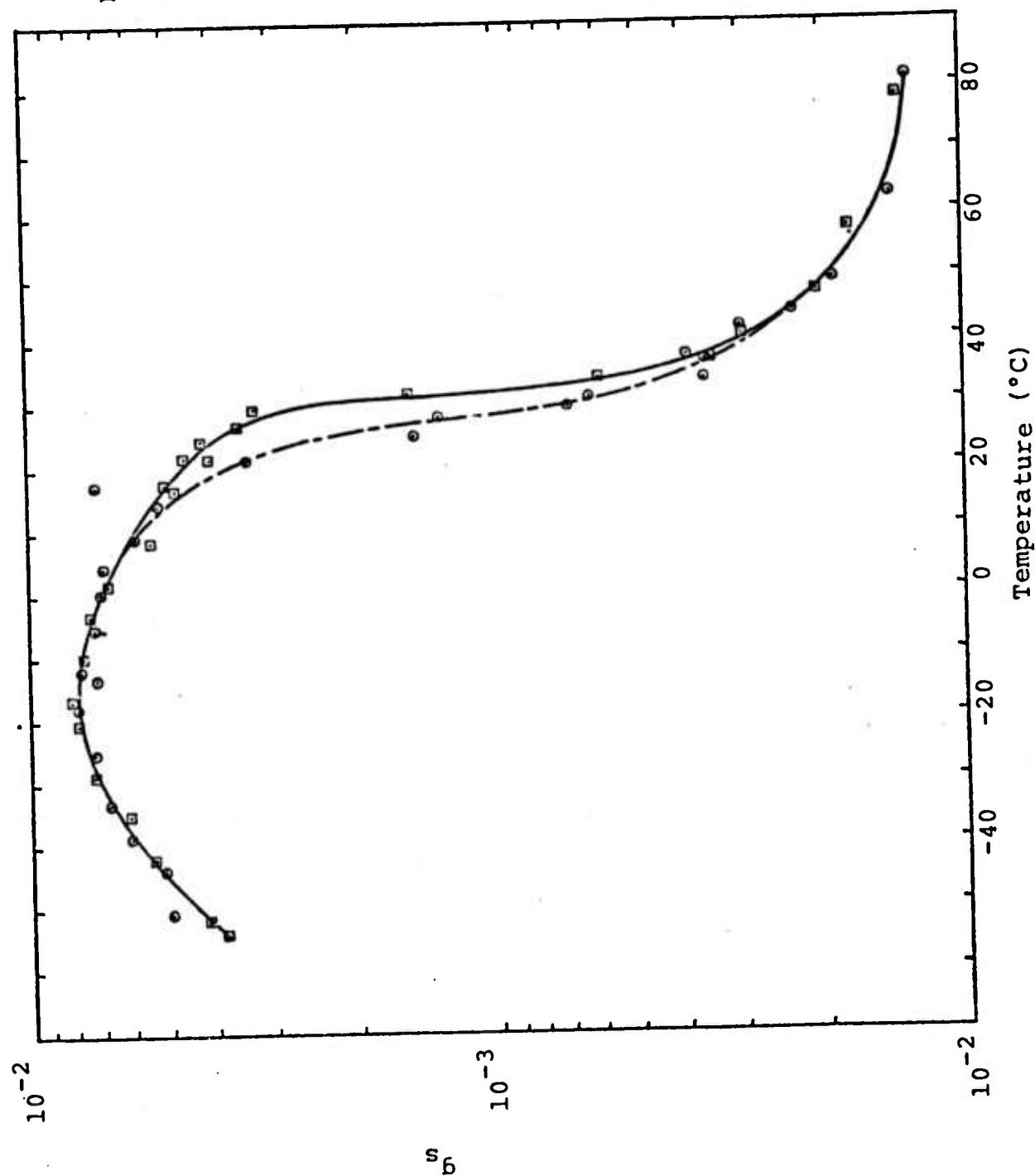


FIGURE 10. Specimen damping factor ( $g_s$ ) as a function of temperature on cooling (for a constant  $y_t = 0.040$  in.).

FIGURE 11. Specimen damping factor ( $g_s$ ) as a function of temperature on both heating and cooling.



$s_b$

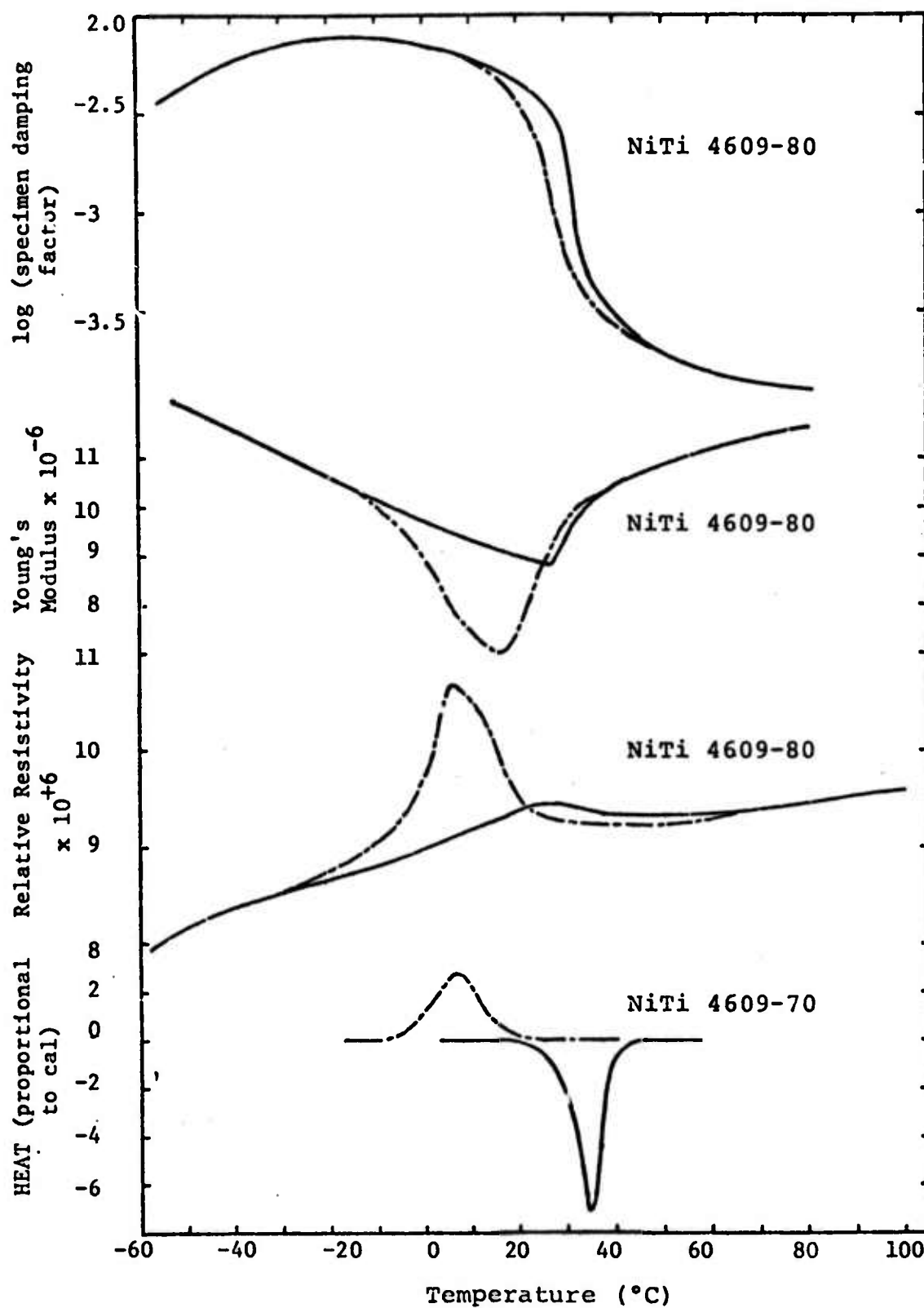


FIGURE 12. Specimen damping factor, Young's modulus, relative resistivity, and heat evolved as a function of temperature for the same series (4609) of the same heat of NiTi.

Measurements of ultrasonic attenuation of the same alloy used in this series are underway. The applied stress is then very small and thus any related shift in  $M_s$  should be minimal. It is expected that by comparing the ultrasonic attenuation results with those obtained with the BBN equipment operating in the 100 to 1000 Hz range, the relative importance of premartensitic damping effects will be clarified.

#### D. Bolt, Beranek and Newman Activities

During the current reporting period, the BBN effort has centered on design, construction, and testing of the Resonant Dwell Apparatus in order to permit determination of specimen loss factor,  $g_s$ , as a function of temperature. The apparatus can now be operated at temperatures between approximately  $-100^\circ\text{C}$  and  $+300^\circ\text{C}$ .

In addition, some determinations of  $g_s$  as a function of temperature have been obtained on standard reed-type and the simplified flat-type specimens.

The measured material loss factors were obtained by means of a resonance dwell apparatus. Heine (4) and Cremer, Heckl and Ungar (5) have discussed resonant measurements of loss factors, and they have discussed a number of other techniques for measuring loss factors. The following discussion is based on their publications.

The resonance dwell technique is a forced vibration method of indirectly determining the loss factors of simple structural elements by measuring their response to excitation at a modal frequency. For a thin beam, where the mode and dynamic stress distributions are well known, the specific damping capacity of the material (energy dissipated per unit volume in one stress cycle at a given peak stress divided by  $2\pi$  times the peak potential energy in the unit volume at the same stress) may be inferred from the determined loss factor.

In this test, the specimen loss factor in a mode (usually the fundamental) is determined from the resonant amplification factor, or  $Q$ , of the specimen in that mode. The mechanical  $Q$  of a

vibrating system is defined in terms of a characteristic deflection  $\delta$  of the system due to distributed exciting forces proportional to the inertia forces of the mode in question. The amplification factor at resonance is

$$Q = \frac{\delta_{\text{res}}}{\delta_0} \quad (1)$$

where  $\delta_0$  is the deflection due to the distributed exciting force being applied statistically and  $\delta_{\text{res}}$  is the deflection when the same pattern of forces is applied in simple harmonic motion at the modal natural frequency. The relationship between  $Q$ , the specimen loss factor  $g_s$ , and the logarithmic decrement  $\zeta$  of single-degree-of-freedom system is

$$\zeta = \frac{\pi}{Q} = \pi g_s \quad (2)$$

The advantages of the resonance-dwell method are: first, the ratio  $\delta_0/\delta_{\text{res}}$ , for a properly designed specimen, is dependent only upon the damping in the specimen; second, the vibrational amplitude  $\delta_{\text{res}}$  may be maintained at any constant level so that specimen damping may be determined as a function of a well-defined stress history; and third, because nothing is attached directly to the vibrating specimen, extraneous energy losses are minimized.

The method for ensuring that the beam specimen is excited at a mode is straightforward. The apparatus is constructed in such a way that the specimen acts as a vibration absorber placed on an excited single degree-of-freedom supporting system (see Figure 13). At a natural frequency of the beam, the response of the supporting system is minimized. The frequency of the response minimum, and hence of the beam mode, can therefore be determined by monitoring the acceleration of the supporting system.

A sketch of the apparatus is shown in Figure 14. A cantilever beam specimen of a test material is clamped to a bar which is connected at one end to an electromagnetic shaker and the other to a heavy base. The thickness of the bar at the base end has been reduced by a saw cut to provide a pivot around which the remainder

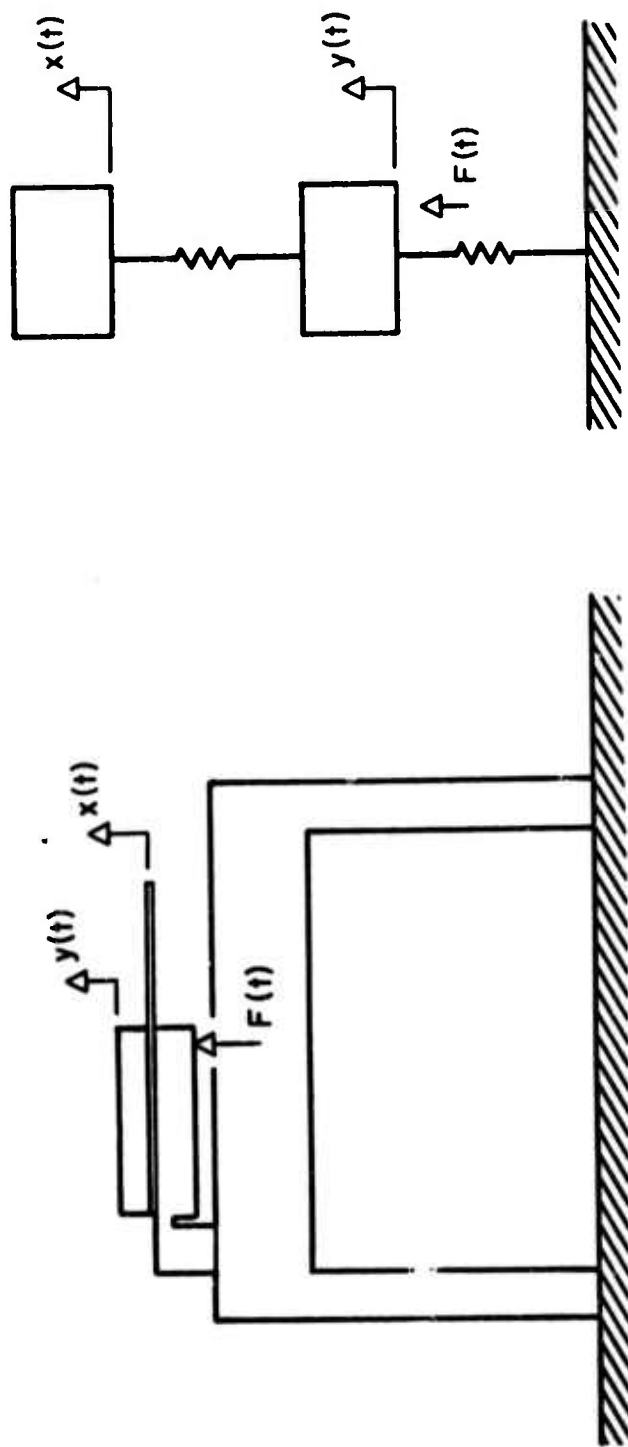


FIGURE 13. AN EXCITED MECHANICAL SYSTEM WITH A RESONANT VIBRATION ABSORBER (EQUIVALENT TO THE RESONANT DWELL DAMPING APPARATUS).



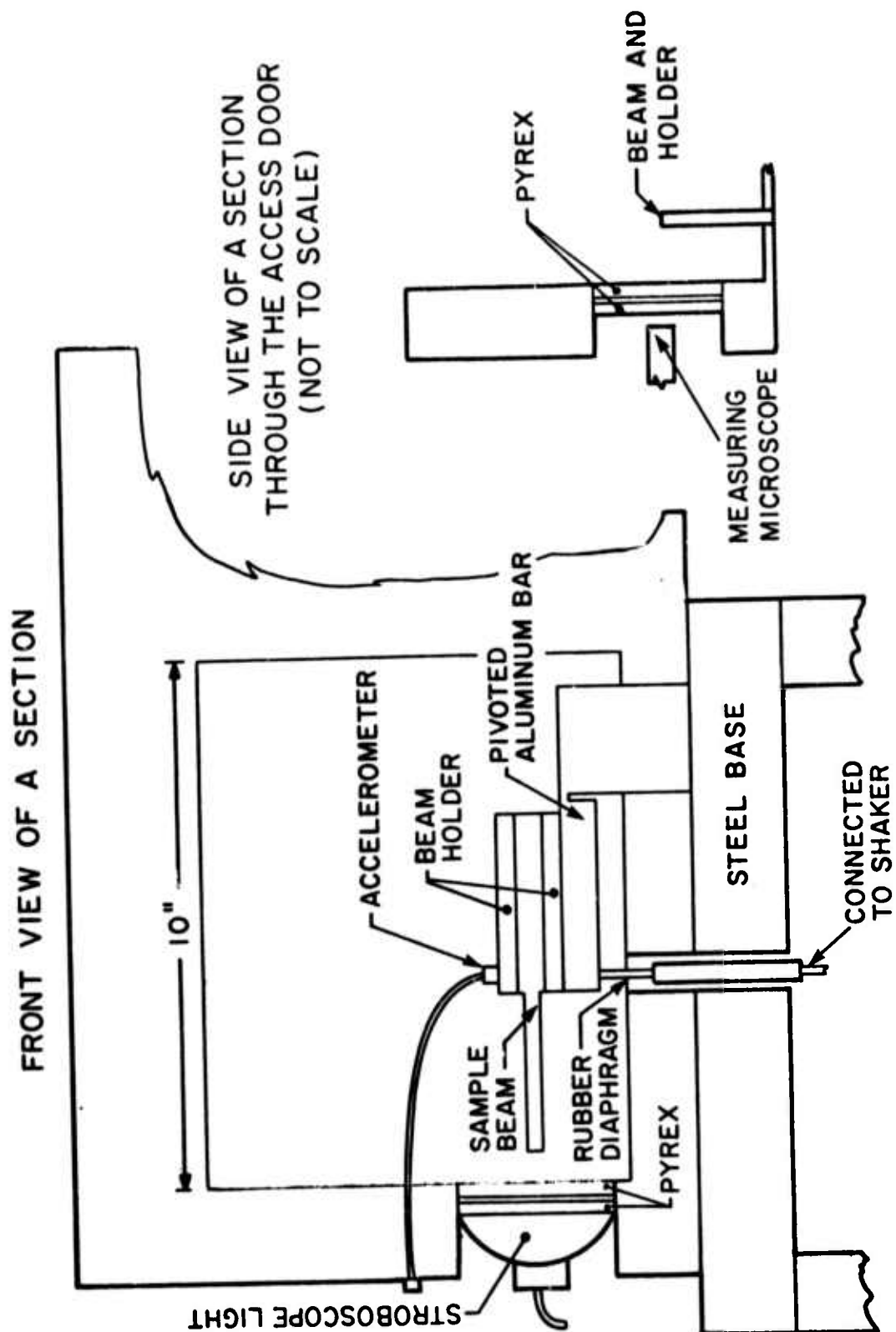


FIGURE 14. SKETCH OF THE RESONANT DWELL APPARATUS AND ENVIRONMENTAL CHAMBER.

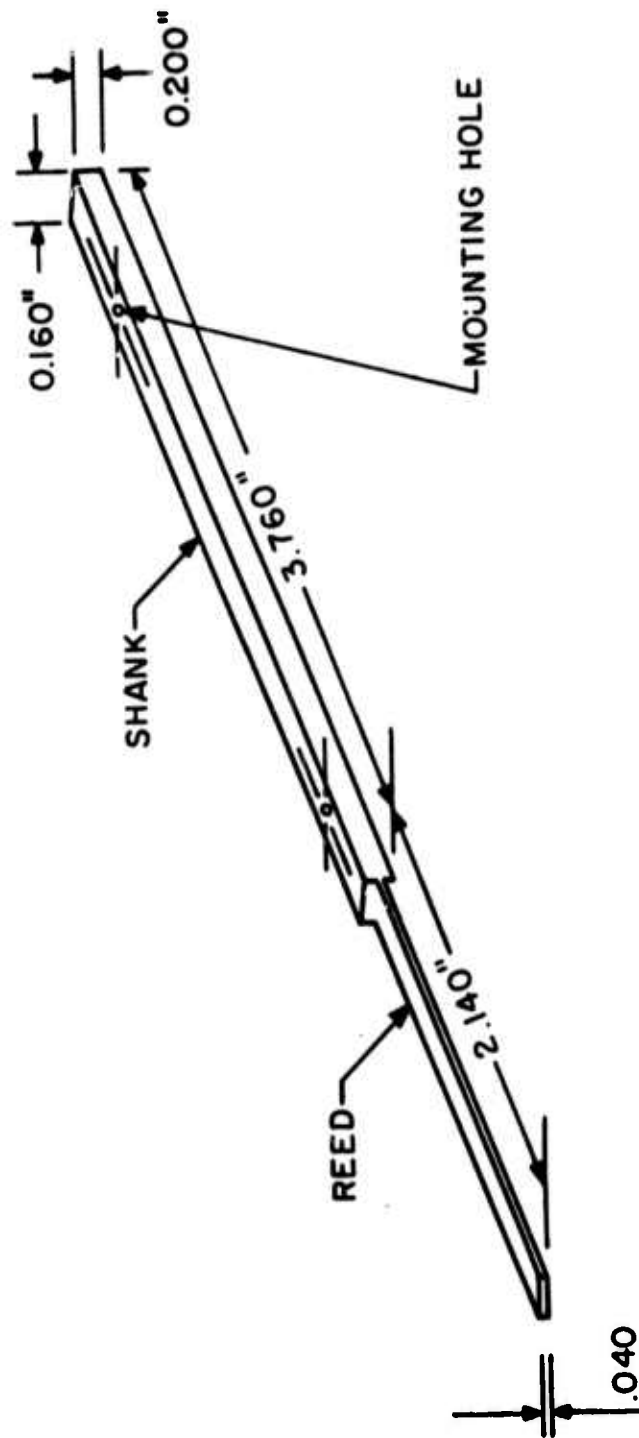


FIGURE 15. SPECIMEN DESIGN FOR MEASURING DAMPING CAPACITY.

of the bar can rotate when excited by the shaker. Figure 15 shows the configuration of a typical reed-type test beam.

The shaker is connected to the bar by a rod which passes through a hole in the base. The hole is sealed by a rubber diaphragm which keeps the gases that are used for temperature control from leaking out of the chamber.

Control of the temperature of the test beam is provided by a commercially-available environmental chamber that has been modified to provide some viewing ports. The chamber can be raised to a temperature of over 600°F by air that is blown over electric heaters. It can be cooled to -100°F by allowing carbon dioxide to expand through the chamber.

The base shown in Figure 14 may be placed on any convenient solid surface, such as a laboratory table. Excitation of the base by the shaker reaction is minimized by the large mass of the base and by supporting the body of the shaker on a jack which passes between the legs of the base. The jack provides some isolation of the shaker from the table. The isolation can be improved by supporting the shaker on a "bridge" that is tied to the floor. Measurements of the acceleration of the base showed the present configuration to be adequate.

The response of the supporting system  $[y(t)]$  in Figure 13] to shaker excitation is measured with an accelerometer mounted on the bar at the root of the specimen. Specimen response  $[x(t)]$  in Figure 13] is measured optically with a low power microscope with a retical.

Figure 16 shows a block diagram of the electronic instrumentation that is used in conjunction with the resonance dwell apparatus. Only two electronic measurements are required--identification of the resonant frequency of the test beam, and accelerometer output. The remaining measurement is the nonelectronic optical measurement of displacement of the beam tip. That measurement is facilitated by the "stop-action" feature of a stroboscope light that is set to flash at nearly the same frequency as the frequency of the mechanical oscillation of the test beam. Figure 17 shows a

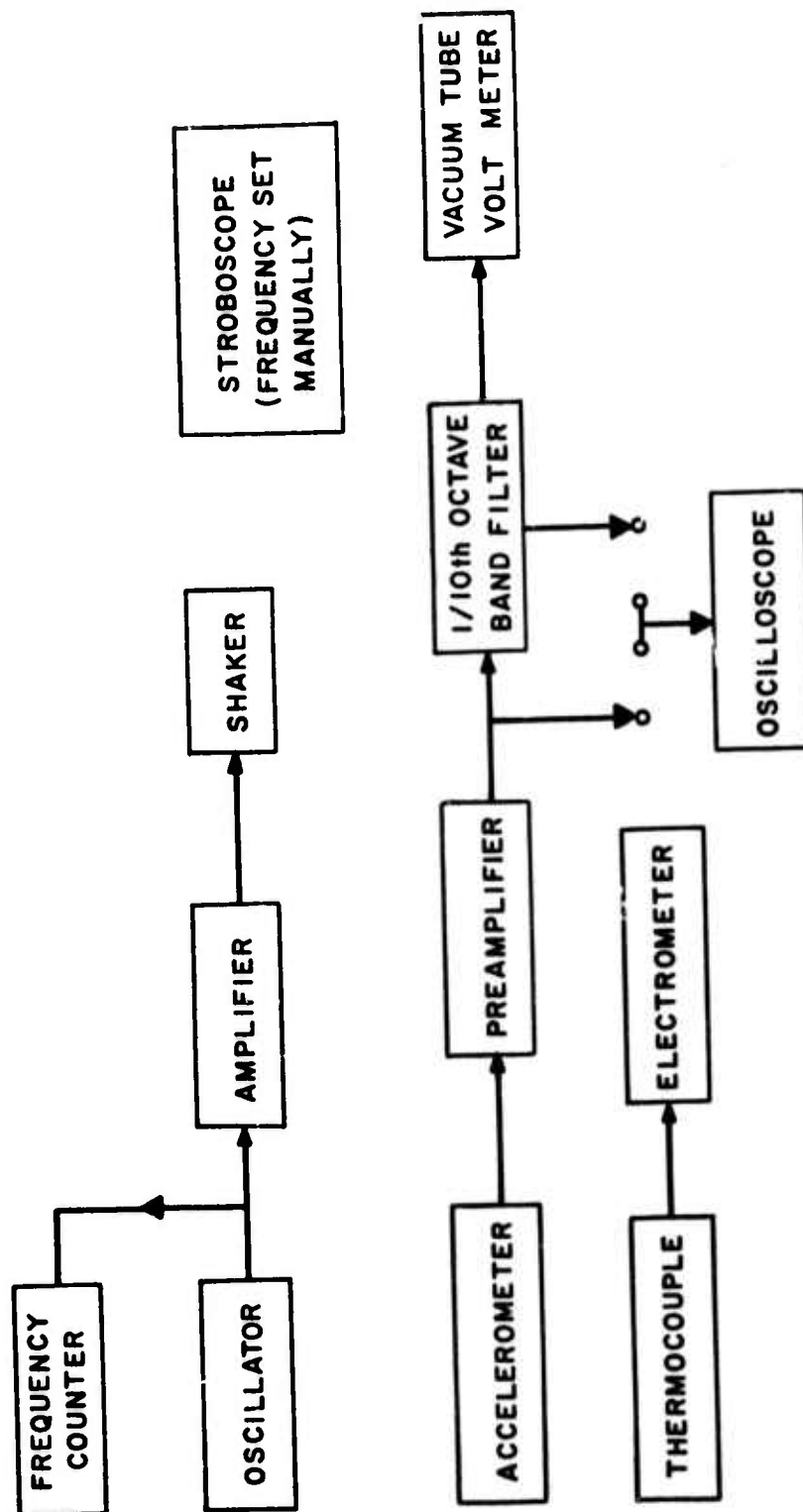
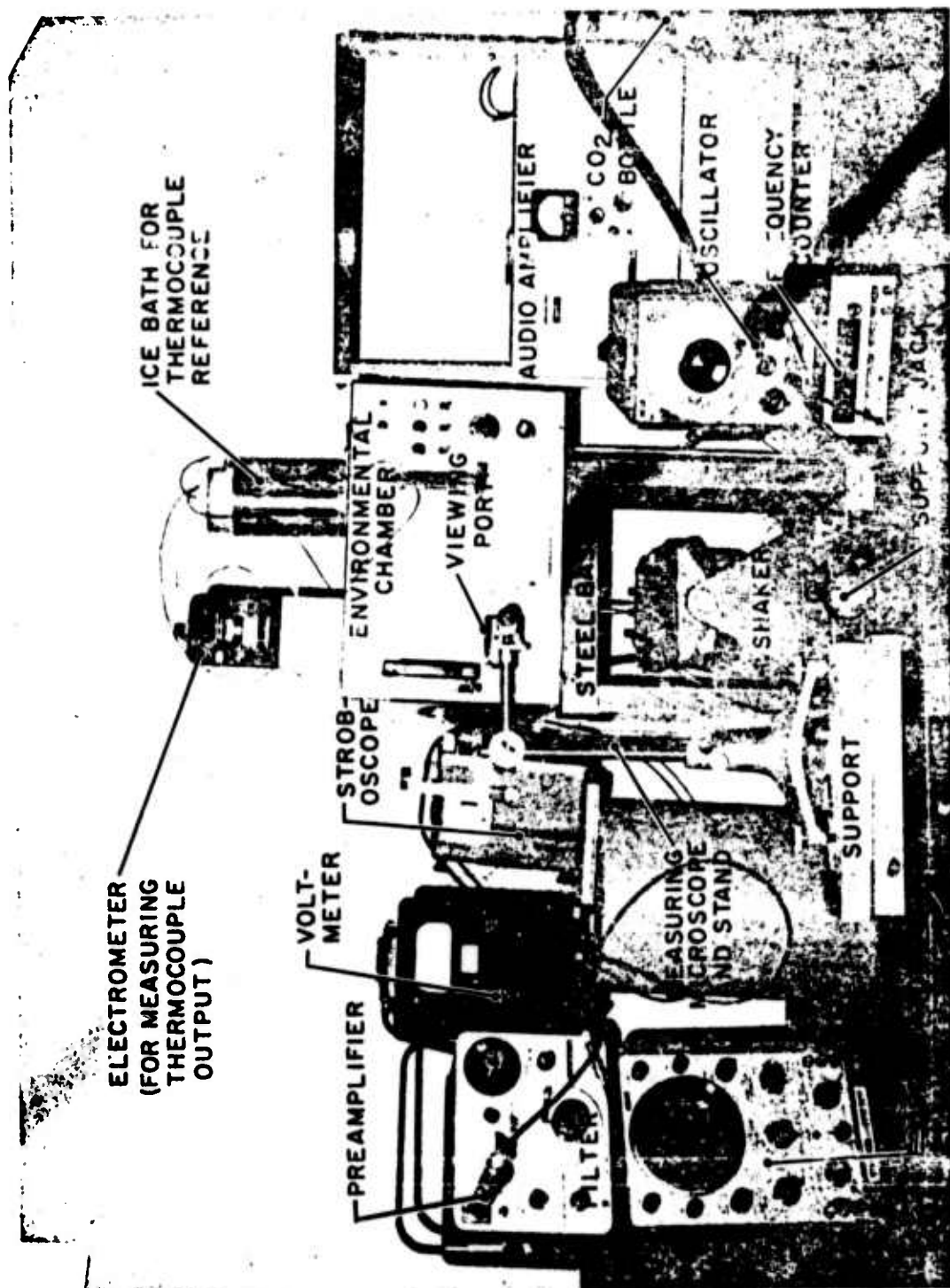


FIGURE 16. BLOCK DIAGRAM OF ELECTRONIC INSTRUMENTATION FOR RESONANT DWELL DAMPING MEASUREMENTS.



Reproduced from  
best available copy.

FIGURE 17. PHOTOGRAPH OF THE ENVIRONMENTAL CHAMBER AND ELECTRONICS COMPRISING THE RESONANT DWELL APPARATUS.

photograph of the environmental chamber and the associated electronics.

The response of a test beam in the resonant dwell apparatus can be described by the following mathematics. For cantilever beams in their fundamental mode of vibration, tip amplitudes as a function of peak stress and specimen natural frequency are given by

$$y_{t,DA} = 3.63 \left( \frac{\sigma_p}{f_n} \right) \frac{1}{\sqrt{E\rho}} \quad (3)$$

where  $y_{t,DA}$  = peak to peak amplitude (in.),  $\sigma_p$  = maximum stress (psi),  $f_n$  = specimen design natural frequency (Hz),  $E$  = Young's Modulus (psi), and  $\rho$  = material density (lb/in<sup>3</sup>). The fundamental natural frequency of a cantilever beam of length  $L$  (in.) and thickness  $h$  (in.) is

$$f_n = \frac{1}{2\pi} \left( \frac{1.8751}{L} \right)^2 h \left( \frac{32E}{\rho} \right)^{1/2} \quad (4)$$

The relationship between the specimen loss factor  $g_s$  and root acceleration  $a_0$ , fundamental specimen frequency  $f_n$ , and beam tip double amplitude  $y_{t,DA}$  is

$$g_s = 0.083 (1 + 0.2L) \frac{a_0}{f_n^2} \frac{1}{y_{t,DA}} \quad (5)$$

where  $a_0$  is the bar acceleration in in./sec<sup>2</sup> measured at the frequency  $f_n$  (the response minimum).

Each beam specimen may be run at the frequencies of modes higher than the fundamental. In practice, however, the highest useful mode is usually the second (though for specially designed specimens the third might be used), because the tip amplitude for a given stress becomes very small with increasing frequency and because the force required for the excitation of a given stress increases with both mode number as well as frequency. For example, a force higher by a factor of more than 3 is required to excite a 10,000 psi peak stress in a specimen with a 650 Hz second mode than

for a specimen designed to have a 650 Hz first mode even though the tip amplitudes required are the same for the two specimens.

The formulas equivalent to Equations 4 and 5 for the second mode are

$$f_2 = \frac{1}{2\pi} \left( \frac{4.6941}{L} \right)^2 h \left( \frac{32E}{\rho} \right)^{1/2} \quad (6)$$

and

$$g_{s,2} = 0.045 (1 + 0.056L) \frac{a_0}{f_{2y,t,DA}^2} \quad (7)$$

The measurements described in this section were obtained with a nickel-titanium reed-type sample like the specimen shown in Figure 17. The test specimen was prepared by heat treatment and stabilized by running it through 70 cycles at ManLabs.

Preliminary measurements of the temperature distribution within the test volume of the commercial temperature chamber revealed that the temperature was not uniform, and the temperature at a given point in the chamber varied with time for a fixed setting of the temperature control. Therefore, it was necessary to measure the temperature of the test specimen by attaching an iron-constantan thermocouple to its surface (near the root of the beam).

These measurements also showed that the specimen loss factor of the nickel-titanium test beam depended on the amplitude of vibration of the tip of the beam at a fixed temperature at which the higher loss factors were exhibited. In addition, the value of the loss factor and the relationship between the loss factor on tip amplitude at a given temperature depended on the past history of the temperature changes. That is, the damping properties at a given temperature were not necessarily the same when the sample was cooling as when it was heating.

The resonant frequency of the test beam varied as the tip amplitude and temperature were changed. Some of the change in loss factor with changing tip amplitude may have been caused by the ac-

companying frequency change, and not by the amplitude change. However, the changes in resonant frequency were small. The resonant frequency of the test beam was between 150 Hz and 200 Hz for the entire range of temperature and tip amplitude covered during the tests.

Figure 18 shows that the specimen loss factor determined from the observations of the test specimen was not a function of tip displacement for the higher temperatures at which lower values of loss factor were observed. Figure 18 also shows that the measured specimen loss factor was a relatively strong function of tip displacement at the lower temperatures at which high specimen loss factors were measured.

The strain-independence of the loss factor at 77°F would seem to rule out dislocation motion and magnetic domain motion as the mechanisms that generate the observed loss factor since those mechanisms are predicted to be stress (and therefore strain) dependent (4). Of the known mechanisms for generating internal friction in metals, theory predicts that only thermal diffusion is independent of stress (*ibid*). Substitution of the values of the thermal coefficients for the test sample into the equation to predict the sample loss factor due to thermal diffusion yielded a value which is an order of magnitude lower than the constant value in Figure 18. Therefore, the loss factor measured at 77°F agrees with no known theory. Either the test material is controlled by some internal loss mechanisms that are not described by available theories, or the measuring equipment introduced some artifact. It seems unlikely that the equipment gave extraneous high readings at 77°F, since readings an order of magnitude lower (in agreement with thermal diffusion theory) were obtained above 100°F.

A number of graphs like those shown in Figure 18 were used to pick off the specimen loss factor corresponding to a constant tip displacement (zero to peak) of .02 in. for various temperatures. It was necessary to use separate graphs for heating sequences and cooling sequences. The value of the loss factor de-



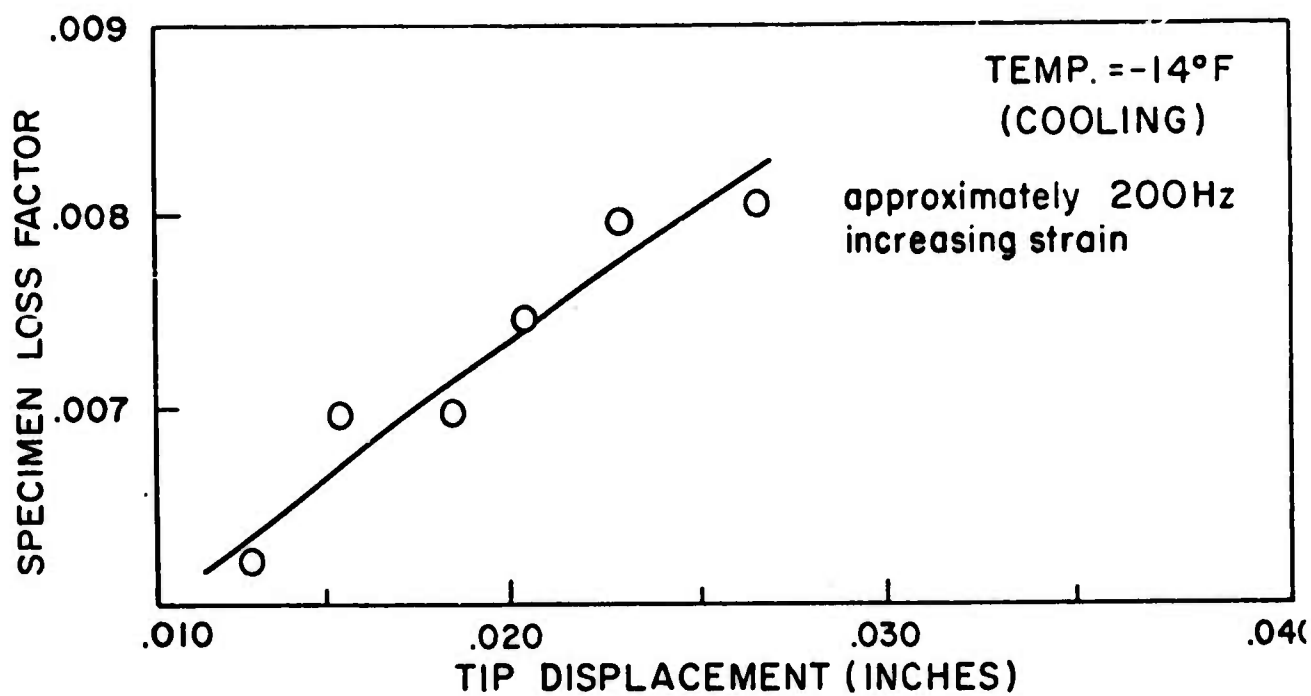
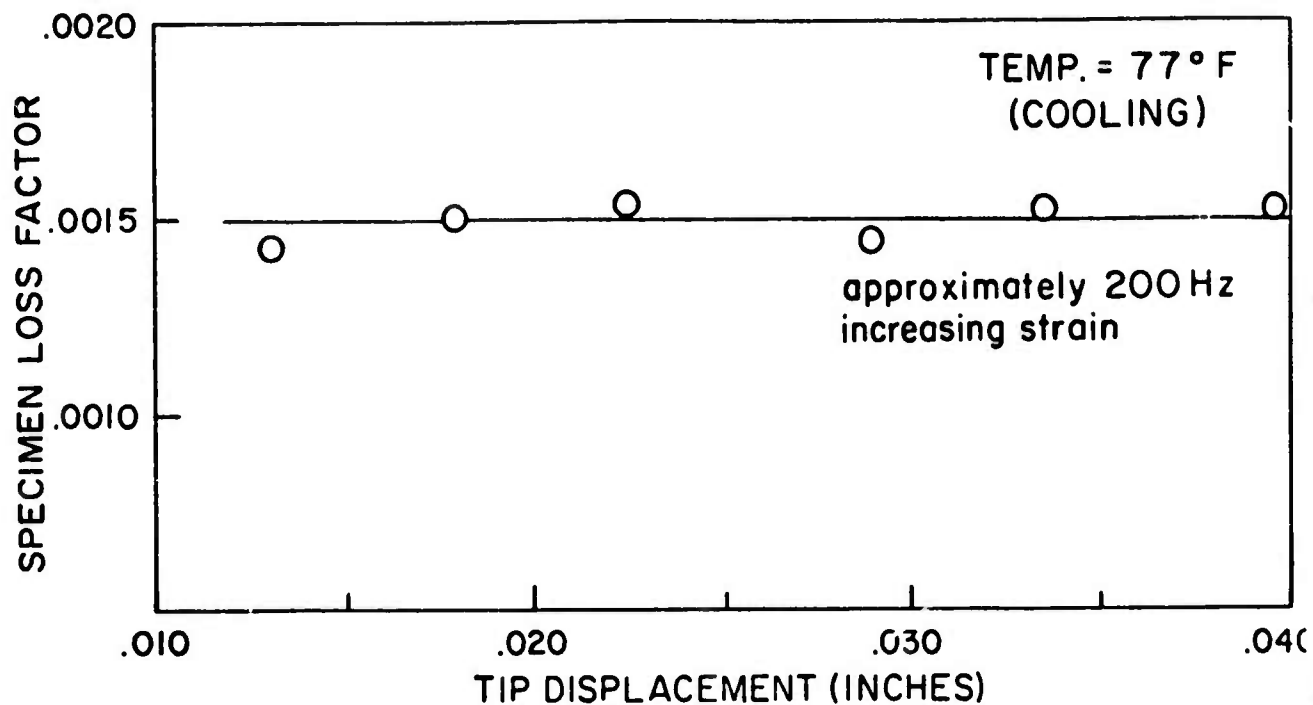


FIGURE 18. AMPLITUDE-DEPENDENCE OF THE SPECIMEN LOSS FACTOR OF NICKEL-TITANIUM SAMPLE NUMBER V4609-80.

pended slightly on the strain sequence (increasing or decreasing strain). Straight lines were fit through the points on the graphs like those in Figure 18. Curved lines may have been equally appropriate. The straight line provided better definition of the temperature dependence of the damping factor than was obtained before any attempt was made to plot the damping factors at constant tip amplitude.

Figure 19 shows the specimen loss factors determined from observations of the nickel-titanium test specimen. The curve reveals some apparent hysteresis in the damping properties of the specimen--the specimen loss factors effective at temperatures near 80°F appeared to be different for the cooling and heating cycles. Relatively small errors in the measured output of the thermocouple attached to the root of the test beam could have contributed to the apparent hysteresis. If portions of the test beam were not at the same temperature that was measured at the root of the beam, there might have been apparent hysteresis generated by the non-uniform temperature of the beam.

The point that lies well above the curve in Figure 19 was determined from observations of the test sample that were made on a different day from the observations that yielded most of the other points in the figure. That point provides some evidence that the response of the test sample depended on the past history of the sample, which is consistent with the observed temperature hysteresis of the damping properties of the test sample.

Laboratory measurements showed that the internal damping of mechanical vibrations of a nickel-titanium test beam was unusually high at temperatures close about 80°F. The specimen loss factor approached .01 near 0°F at about 200 Hz and about 5000 psi stress. That value for the loss factor is more typical of built-up composite structures than homogeneous samples (6,7). The values of the loss factor determined from the measurements depended on temperature, past history of temperature, the amplitude of the tip of the vibrating test reed, possibly upon the resonant frequency of the test beam, and depended slightly upon the strain history of

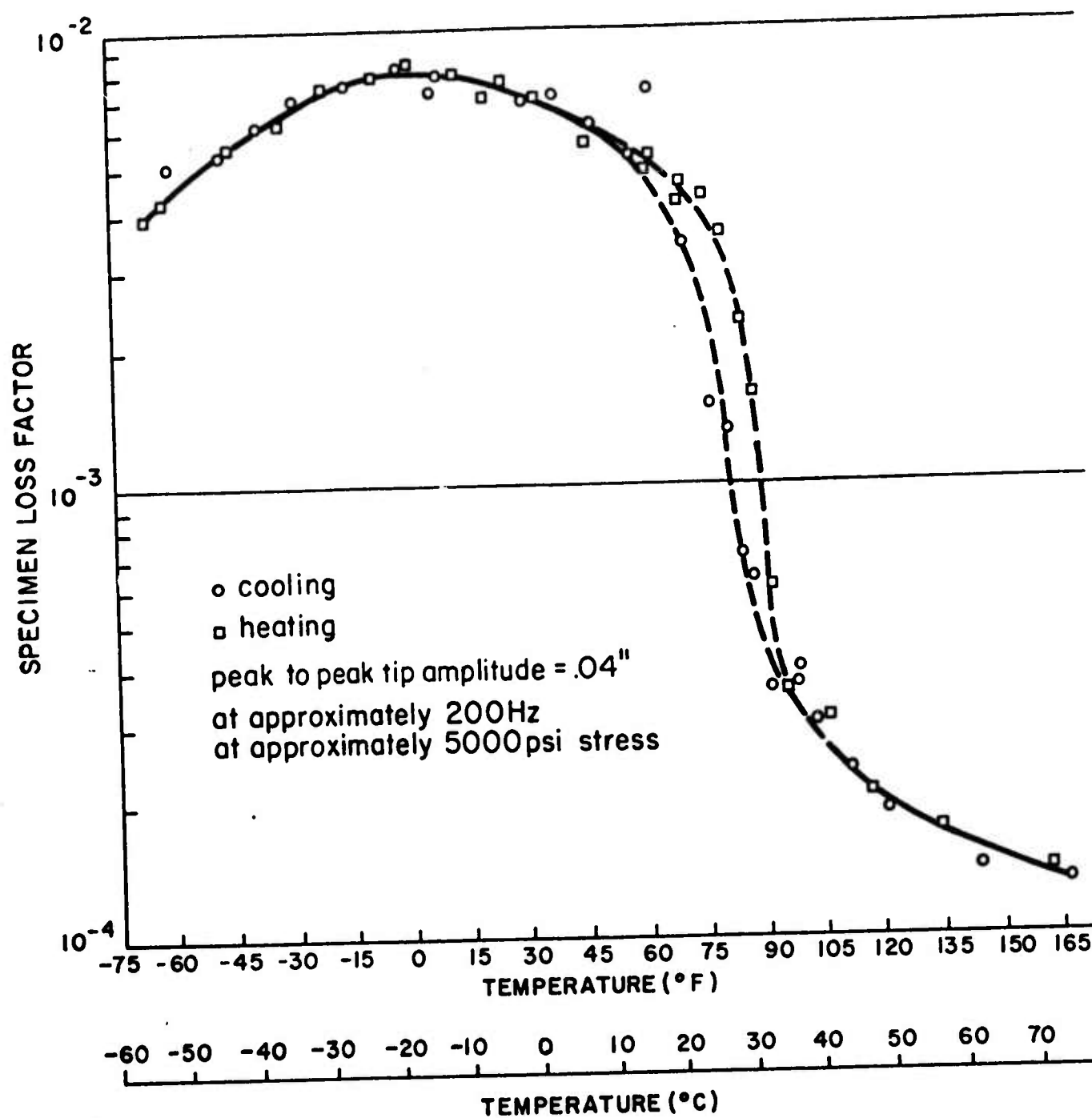


FIGURE 19. TEMPERATURE-DEPENDENCE OF THE SPECIMEN LOSS FACTOR OF NICKEL-TITANIUM SAMPLE NUMBER V4609-80 (AT CONSTANT TIP AMPLITUDE).

of the test beam.

Some of the experimental data do not agree with theories of the mechanisms of generation of internal friction. Although equipment artifacts cannot be ruled out, it seems unlikely that extraneous equipment responses were responsible for the unexpected data.

There is a possibility that the apparent temperature hysteresis of the specimen loss factor described in this report was due to slight errors in the measurements of the temperature of the test beam. In addition, it is possible that the temperature of the test beam was not uniform during the tests. The beam and test chamber should be provided with a number of thermocouples in order to precisely define the thermal conditions of the test beam.

The question of the origin of those particular data which do not conform to theory should be resolved. If the appropriate stress range can be covered for several samples of different dimensions but identical material, then there would be more basis for deciding whether to look for equipment artifacts or to revise the theories.

It is possible that the loss factor of the test sample at a given temperature and a given level of stress or strain is a function of the resonant frequency of the beam (4). In addition, temperatures and/or stress hysteresis might be more pronounced at frequencies and stresses other than those for which the reported measurements were gathered. If several samples of different lengths and thicknesses can be prepared from a single batch of Ni-Ti alloy, then curves of loss factor versus increasing and decreasing temperature can be prepared for several combinations of frequency and stress level. Moreover, since the loss factor of the test specimen depends not only on the temperature sequence leading up to a given test temperature, but upon the length of time that the sample is maintained at a given test temperature as well, it would be instructive to investigate the temperature dependence of the loss factor for different rates of increasing and decreasing the temperature.

E. Summary of Work to Date

The objective of this interdisciplinary program is to obtain a basic understanding of the mechanism of high internal damping in alloys which undergo certain martensitic-type transformations and thereby to identify potential structural materials approaches for use in noise and vibration abatement applications.

At present NiTi, Cu-Al-Ni and Fe-Pt alloys are being studied to determine damping capacity as a function of temperature both above and below the  $M_s$  temperature. Measurements of heat capacity and transformation characteristics have been completed for NiTi and one Fe-Pt alloy and are in progress for a second Fe-Pt alloy and the Cu-Al-Ni alloy. Mechanical property measurements and assessment of the effects of elastic and plastic strains on the characteristics of the Ni-Ti alloy are in progress.

It was found that the martensitic transformation in NiTi alloys is of the thermoelastic type. Evidence was obtained which indicated a large increase in internal damping capacity at temperatures associated with the premartensitic or "soft-mode" temperature regime. Experiments completed during the past three months have confirmed these findings. Moreover it was found that plastic deformation can be employed to substantially alter the transformation characteristics. Consequently it is anticipated that a corresponding change in damping characteristics is attainable. It was also determined that the damping capacity in Fe-Pt alloys is directly related to the amount of ordering in the parent phase.

### References

1. G. D. Sandrock, Met. Tr. (1974) 5 299.
2. G. D. Sandrock, A. J. Perkins and R. F. Heheman, Met. Tr. (1971) 2 2769.
3. K. Otsuka, T. Sawamura, K. Shimuzu and C. M. Wayman, Met. Tr. (1971) 2 2583.
4. J. C. Heine, "The Stress and Frequency Dependence of Material Damping on Some Engineering Alloys," Ph.D. Dissertation, Massachusetts Institute of Technology (1966).
5. L. Cremer, M. Heckl and E. E. Ungar, Structure-Borne Sound, Springer-Verlag, New York, Chapter III (1973).
6. E. E. Ungar, "Damping of Panels," in Noise and Vibration Control, Ed. Leo. L. Beranek, McGraw-Hill, New York (1971).
7. E. E. Ungar, "The Status of Engineering Knowledge Concerning the Damping of Built-up Structures," J. Sound & Vib. 26, (1), 141-154 (1973).